

A Prospect-Theoretic Policy Gradient Algorithm for Behavioral Alignment in Reinforcement Learning

Olivier Lepel* Anas Barakat*

February 28, 2025

Abstract

Classical reinforcement learning (RL) typically assumes rational decision-making based on expected utility theory. However, this model has been shown to be empirically inconsistent with actual human preferences, as evidenced in psychology and behavioral economics. Cumulative Prospect Theory (CPT) provides a more nuanced model for human-based decision-making, capturing diverse attitudes and perceptions toward risk, gains, and losses. While prior work has integrated CPT with RL to solve a CPT policy optimization problem, the understanding and practical impact of this formulation remain limited. We revisit the CPT-RL framework, offering new theoretical insights into the nature of optimal policies. We further derive a novel policy gradient theorem for CPT objectives, generalizing the foundational result in standard RL. Building on this theorem, we design a model-free policy gradient algorithm for solving the CPT-RL problem and demonstrate its performance through simulations. Notably, our algorithm scales better to larger state spaces compared to existing zeroth-order methods. This work advances the integration of behavioral decision-making into RL.

1 Introduction

In classical reinforcement learning (RL), rational agents make decisions to maximize their expected cumulative rewards through interaction with their environment. This paradigm is primarily guided by expected utility theory, which has long been the dominant framework for decision-making under risk. Within this framework, agents are generally considered to be risk-neutral; however, risk-seeking and risk-averse behaviors can also be modeled by modifying the utility function, thereby adjusting the policy optimization objective (see e.g. Prashanth et al. [2022] for a survey).

While risk-sensitive RL extends beyond risk-neutral settings to capture individual risk preferences (using e.g. variance or conditional value at risk metrics), it remains limited in fully representing the complexities of human decision-making and fail to capture the psychological nuances of how humans perceive risks, gains, and losses, often leading to decisions misaligned with human preferences. Specifically, risk-sensitive RL fails to account for the asymmetric perception of gains and losses, as well as the probability distortions inherent in human cognition, such as the tendency to overestimate rare events and underestimate frequent ones (see appendix B for an illustration in a simulation). These psychological and cognitive biases, critical to understanding real-world human decisions under uncertainty, are beyond the scope of traditional risk-sensitive RL frameworks, necessitating a more comprehensive approach.

Cumulative Prospect Theory (CPT), developed by the pioneering behavioral psychologist Daniel Kahneman¹ together with his colleague Amos Tversky in their seminal works combining cognitive psychology and economics [Kahneman and Tversky, 1979, Tversky and Kahneman, 1992], provides a more

*Most of this work was completed when the authors were both affiliated with the department of computer science at ETH Zürich, Switzerland, O.L. as a Master student and A.B. as a postdoctoral researcher. A.B. is now affiliated with Singapore University of Technology and Design as a research fellow. Contact: barakat9anas@gmail.com.

¹Daniel Kahneman has been awarded the Nobel Prize in Economic Sciences in 2002 ‘for having integrated insights from psychological research into economic science, especially concerning human judgment and decision-making under uncertainty’.

nuanced understanding of human decision-making to explain several empirical observations invalidating the standard expected utility theory. CPT models how individuals perceive outcomes asymmetrically, being risk-averse in the domain of gains and risk-seeking in the domain of losses, and distort probabilities to reflect cognitive biases. These insights have led to widespread applications of CPT in stateless static settings in high-stakes domains such as healthcare in psychiatry [Sip et al., 2018, George et al., 2019, Mkrtchian et al., 2023], chronic diseases treatment [Zhao et al., 2023] and emergency decision making [Sun et al., 2022] where taking into account psychological factors is of paramount importance, as well as other application domains such as energy [Ebrahimigharehbaghi et al., 2022, Dorahaki et al., 2022] and finance [Ladrón de Guevara Cortés et al., 2023, Luxenberg et al., 2024] to name a few. However, these applications often overlook the sequential decision-making nature inherent in many real-world problems, where the outcome of one decision can affect future choices, a critical aspect of RL.

The integration of CPT into RL provides a promising avenue for behaviorally-aligned sequential decision-making, as it allows RL agents to consider both risk preferences and probability distortions in dynamic environments. While a few isolated recent works have explored this integration [L.A. et al., 2016, Borkar and Chandak, 2021, Ramasubramanian et al., 2021, Danis et al., 2023], the understanding and practical impact of CPT in RL remains limited. Specifically, the computational challenges and theoretical underpinnings of CPT-based RL models are still underexplored, and the practical effectiveness of such models in sequential decision-making problems is not well understood.

In this work, we focus on the policy optimization problem where the objective is the CPT value of the cumulative sum of rewards, induced by a parametrized policy in a Markov Decision Process. Our main contributions are as follows:

About optimal policies in CPT-RL. We provide theoretical insights about the nature of an optimal policy for CPT policy optimization. Unlike in standard MDPs where policies are typically Markovian, an optimal policy is stochastic and non-Markovian in general. When we set the probability distortion function to identity, we show that the policy search set can be significantly reduced to a much smaller policy class when solving (CPT-PO). In this same setting, we also characterize a family of utility functions (affine and exponential utility functions) for which the CPT value objective can be maximized with a Markovian policy. However, we prove that this characterization does not hold anymore when considering nontrivial probability distortion and (nonlinear) utilities together in (CPT-PO).

Policy gradient theorem for CPT-RL. We establish a policy gradient theorem providing a closed form expectation expression for the gradient of our CPT-value objective w.r.t. the policy parameter under suitable regularity conditions on the utility and probability distortion functions. This result generalizes the standard policy gradient theorem in RL.

Policy gradient algorithm for CPT-RL. Building on our policy gradient theorem, we design a policy gradient algorithm to solve the CPT policy optimization problem. The stochastic policy gradient we use involves a novel integral term to be computed and we propose a tailored Monte Carlo estimation procedure to approximate it. We perform simulations to illustrate our theoretical results on simple examples. In particular, we test our PG algorithm in two CPT-RL applications: a traffic control application with finite discrete state action spaces and an electricity management task in a continuous state action setting. We also compare the performance of our PG algorithm to the previously proposed zeroth order algorithm to show the robustness and scalability of our algorithm to higher dimensional MDPs.

2 From Classical RL to CPT-RL

Markov Decision Process. A discrete-time Markov Decision Process (MDP) [Puterman, 2014] is a tuple $\mathcal{M} = (\mathcal{S}, \mathcal{A}, \mathcal{P}, r, \rho)$, where \mathcal{S}, \mathcal{A} are respectively the state and action spaces, supposed to be finite for simplicity, $\mathcal{P} : \mathcal{S} \times \mathcal{A} \times \mathcal{S} \rightarrow [0, 1]$ is the state transition probability kernel, and $r : \mathcal{S} \times \mathcal{A} \rightarrow [-r_{\max}, r_{\max}]$ is the reward function which is bounded by $r_{\max} > 0$, ρ is the initial state probability distribution. A randomized stationary Markovian policy, which we will simply call a policy, is a mapping $\pi : \mathcal{S} \rightarrow \Delta(\mathcal{A})$ which specifies for each $s \in \mathcal{S}$ a probability measure over the set of actions \mathcal{A} by $\pi(\cdot|s) \in \Delta(\mathcal{A})$ where

$\Delta(\mathcal{A})$ is the simplex over the finite action space \mathcal{A} . Each policy π induces a discrete-time Markov reward process $\{(s_t, r_t := r(s_t, a_t))\}_{t \in \mathbb{N}}$ where $s_t \in \mathcal{S}$ represents the state of the system at time t and r_t corresponds to the reward received when executing action $a_t \in \mathcal{A}$ in state $s_t \in \mathcal{S}$. We denote by $\mathbb{P}_{\rho, \pi}$ the probability distribution of the Markov chain $(s_t, a_t)_{t \in \mathbb{N}}$ generated by the MDP controlled by the policy π with initial state distribution ρ . We use $\mathbb{E}_{\rho, \pi}$ (or often simply \mathbb{E} instead) to denote the expectation w.r.t. the distribution of the Markov chain $(s_t, a_t)_{t \in \mathbb{N}}$. At each time step $t \geq 0$, the agent follows its policy π by selecting an action a_t drawn from the action distribution $\pi_t(\cdot | s_t)$ where s_t is the environment state at time t . Then the environment transitions to a state s_{t+1} sampled from the state distribution $\mathcal{P}(\cdot | s_t, a_t)$ given by the state transition kernel \mathcal{P} and the agent obtains a reward r_t . In traditional RL, the goal of the agent in MDPs is to find a policy π maximizing the expected cumulative rewards, i.e. the so-called expected return $J(\pi) := \mathbb{E}_{\rho, \pi}[\sum_{t=0}^{H-1} r_t]$ where s_0 follows the initial state distribution ρ and $H \geq 1$ is a finite horizon.

Policy classes. We now introduce different sets of policies which will be important for stating our results. Each policy class is defined according to the information history the policies have access to for selecting actions. Here, a history $h_t \in \mathcal{H}$ is a finite sequence of successive states, actions and rewards: $(s_0, a_0, r_0, \dots, s_{t-1}, a_{t-1}, r_{t-1})$.² More specifically, throughout this work, we will consider the following sets of policies: $\Pi_{NM} := \{\mathcal{H} \rightarrow \Delta(\mathcal{A})\}$ is the set of non-(necessarily)Markovian policies, $\Pi_{\Sigma, NS} := \{\mathcal{S} \times \mathbb{R} \times \mathbb{N} \rightarrow \Delta(\mathcal{A})\}$ is the set of policies that only depend on the current state, the timestep and the sum of rewards accumulated so far (i.e. $\pi(s, \sum_{k=0}^{t-1} r_k, t)$), $\Pi_{\Sigma, S} := \{\mathcal{S} \times \mathbb{R} \rightarrow \Delta(\mathcal{A})\}$ is the set of policies that only depend on the state and the sum of rewards (i.e. $\pi(s, \sum_{k=0}^{t-1} r_k)$), $\Pi_{M, NS} := \{\mathcal{S} \times \mathbb{N} \rightarrow \Delta(\mathcal{A})\}$ is the set of Markovian policies (i.e. $\pi(s, t)$) and $\Pi_{M, S} := \{\mathcal{S} \rightarrow \Delta(\mathcal{A})\}$ is the set of stationary Markovian policies, i.e. Markovian policies which are time-independent. Deterministic policies assign a single action to each state. For each set of policies defined above, we define their corresponding subset of deterministic policies: $\Pi_{NM}^D, \Pi_{\Sigma, NS}^D, \Pi_{\Sigma, S}^D, \Pi_{M, NS}^D$ and $\Pi_{M, S}^D$.

Remark 1. $\Pi_{M, S} \subseteq \Pi_{M, NS} \subseteq \Pi_{\Sigma, NS} \subseteq \Pi_{NM}$ and $\Pi_{M, S} \subseteq \Pi_{\Sigma, S} \subseteq \Pi_{\Sigma, NS} \subseteq \Pi_{NM}$ (see Fig. 4, App. A).

Cumulative Prospect Theory Value. Instead of the expected return, CPT prescribes to consider the CPT value which will be defined in this paragraph. As previously mentioned, CPT relies on three distinct elements which we further detail in the following:

(a) **A reference point.** The human agent has a reference attainable reward value in comparison to which they evaluate their possible reward outcomes. Rewards larger than the reference are perceived as gains whereas lower values are viewed as losses.

(b) **A utility function $\mathcal{U} : \mathbb{R} \rightarrow \mathbb{R}_+$.** The agent’s utility is a continuous and non-decreasing function which is not necessarily linear w.r.t. the total reward received by the agent. We consider the function $u^+ : \mathbb{R} \rightarrow \mathbb{R}_+$ describing the gains and defined for every $x \in \mathbb{R}$ by $u^+(x) = \mathcal{U}(x)$ if $x \geq x_0$ and zero otherwise. Similarly, the function $u^- : \mathbb{R} \rightarrow \mathbb{R}_+$ which encodes the losses is defined by $u^-(x) = -\mathcal{U}(x)$ if $x \leq x_0$ and zero otherwise. Here, x_0 denotes the reference point. Typically, the utility function is concave (respectively convex) for positive (resp. negative) rewards w.r.t. the reference point, i.e. u^+ is concave on \mathbb{R}_+ and $-u^-$ is convex on \mathbb{R}_- . For concreteness, we will use [Kahneman and Tversky \[1979\]](#)’s utility function as a running example: $\mathcal{U}(x) = (x - x_0)^\alpha$ if $x \geq x_0$ and $\mathcal{U}(x) = -\lambda(x - x_0)^\alpha$ if $x < x_0$, where $\lambda = 2.25, \alpha = 0.88$ are recommended hyperparameters. See Fig. 8 for an illustration with $x_0 = 0$.

(c) **A probability distortion function $w : [0, 1] \rightarrow [0, 1]$.** This is a continuous non-decreasing weight function that distorts the probability distributions of the gain and loss variables. This function typically captures the human tendency to overestimate the probability of rare events and underestimate the probability of more certain ones. Similarly to the utility function, we denote by w^+ (resp. w^-) the function that warps the cumulative distribution function for gains (resp. for losses). Both functions are required to be defined on $[0, 1]$, with values in $[0, 1]$ and to be non-decreasing, continuous, with $w^+(0) = w^-(0) = 0$ and $w^+(1) = w^-(1) = 1$. Examples of such weights functions in the literature include $w : p \mapsto p^\eta(p^\eta + (1-p)^\eta)^{-\frac{1}{\eta}}$ [[Kahneman and Tversky, 1979](#)] and $w : p \mapsto \exp(-(-\ln p)^\eta)$ [[Prelec,](#)

²Rewards can be discarded from the history when they are deterministic functions of state-action pairs.

1998] where $\eta \in (0, 1)$ is a hyperparameter. We refer the reader to appendix F.2 for examples and plots of utility and probability weight functions.

The CPT value of a real-valued random variable X is

$$\mathbb{C}(X) = \int_0^{+\infty} w^+(\mathbb{P}(u^+(X) > z))dz - \int_0^{+\infty} w^-(\mathbb{P}(u^-(X) > z))dz, \quad (1)$$

where appropriate integrability assumptions are assumed. While the CPT value $\mathbb{C}(X)$ accounts for the human agent’s distortions in perception, it also recovers the expectation $\mathbb{E}(X)$ with weight functions w^+, w^- and utility functions u^+ (resp. $-u^-$) restricted to \mathbb{R}_+ (resp. \mathbb{R}_-) are set to be the identity functions. In addition, several risk measures such as variance, Conditional Value at Risk (CVar) and distortion risk measures are also particular cases of CPT values with *discontinuous* probability weighting functions (at a single point). See appendix F for proofs of these facts and Table 1 therein for a synthetic view of the settings captured by CPT. Note that VaR and CVar are rooted in the financial risk management literature and rely on objective probability distributions whereas CPT originates from behavioral economics and focuses on subjective risk perception and decision-making.

Problem formulation: CPT-RL. In this work, we will focus on the policy optimization problem where the objective is the CPT value of the random variable $X = \sum_{t=0}^{H-1} r_t$ recording the cumulative rewards induced by the MDP and the policy π for the finite horizon $H \geq 1$:

$$\max_{\pi \in \Pi_{NM}} \mathbb{C} \left[\sum_{t=0}^{H-1} r_t \right]. \quad (\text{CPT-PO})$$

We will also be concerned with the particular case of (CPT-PO) in which w^+, w^- are set to the identity, namely the expected utility objective where only returns are distorted by the utility function:

$$\max_{\pi \in \Pi_{NM}} \mathbb{E} \left[\mathcal{U} \left(\sum_{t=0}^{H-1} r_t \right) \right]. \quad (\text{EUT-PO})$$

Similar problem variants for total cost and infinite horizon discounted settings can also be formulated. Notice that standard RL policy optimization problems are clearly particular cases of (CPT-PO).

Example: Personalized Treatment for Pain Management. We illustrate our problem formulation with a concrete example in healthcare to give the reader more intuition about the different features of CPT-RL, its importance in applications when human perception and behavior matter and its differences compared to risk-sensitive RL. The goal is to help a physician manage a patient’s chronic pain by suggesting a personalized treatment plan over time. The challenge here is to balance pain relief and the risk of opioid dependency or other side effects that might be due to the treatment, i.e. short-term relief and longer term risks. We propose to train a CPT-RL agent to help the physician.

1. **Why sequential decision making?** (a) The physician needs to adjust treatment at each time step depending on the patient’s reported pain level as well as the observed side effects. This is relevant to dynamic treatment regimes in general (such as for chronic diseases, see e.g. Yu et al. [2021] for a survey) in which considering delayed effects of treatments is also important (and RL does account for such effects). (b) Decisions clearly impact the patient’s immediate pain relief, dependency risks in the future and their overall health condition. A state is described by e.g. current pain level, dependency risk and side effect severity. Actions are treatments, e.g. no treatment, alternative treatment or opioid treatment.
2. **Why CPT-RL?** Patients and clinicians make decisions influenced by psychological biases. We illustrate the importance of each one of the three features of CPT in section 2 (reference point, utility and probability distortion weight functions) via this example:
 - *Reference points:* Patients assess and report pain levels according to their subjective (psychologically biased) baseline. Incorporating reference point dependence leads to a more realistic model of

human decision-making taking into account *perceived* gains and losses. In our example, reducing pain from a level of 7 to 5 is not perceived the same way if the reference point of the patient is 3 or 5. In contrast, risk-sensitive RL treats every pain reduction as a uniform gain, regardless of the patient’s starting reference pain level.

- *Utility transformation:* Patients might often show a loss averse behavior, i.e., they might perceive pain increase or withdrawal symptoms as worse than equivalent gains in pain relief. Note here that loss aversion should not be confused with risk aversion [Schmidt and Zank, 2005]. In short, loss aversion can be defined as a *cognitive bias* in which the emotional impact of a loss is more intense than the satisfaction derived from an equivalent gain. For instance, in our example, a 2-point increase in pain might be seen as much worse than a 2-point reduction even if the change is the same in absolute value. This loss aversion concept is a cornerstone of Kahneman and Tversky’s theory. In contrast, risk aversion rather refers to the *rational* behavior of undervaluing an uncertain outcome compared to its expected value. Risk sensitive approaches might be less adaptive to a patient’s subjective preferences if they deviate from objective risk assessments.
 - *Probability weighting:* Low probability events such as severe side effects (e.g., opioid overdose or dependency) might be overweighted or underweighted based on the patient’s psychology.
3. **CPT-RL vs Risk-averse RL.** In terms of policies, risk-averse RL would favor non-opioid treatments unless extreme pain levels make opioids justifiable. In contrast, CPT-RL policies would prescribe opioids if pain significantly exceeds the patient’s reference point. As dependency risk increases, CPT-RL policies would transition to non-opioid treatments as a consequence of overweighting the probability of rare catastrophic outcomes. Notably, CPT-RL policies can oscillate between risk-seeking (to address high pain) and risk-averse (to avoid severe side effects). In contrast, a risk-sensitive agent focuses on minimizing variability in health states and dependency risks and would likely avoid opioids in most cases unless pain levels become extreme. Such risk-sensitive policies favor stable strategies (e.g., consistent non-opioid use), prioritizing low variance in patient outcomes.

Scope of this work. Several behavioral studies model the reference points, utility and probability weight functions using real patient treatment data [Mkrtchian et al., 2023, George et al., 2019, Sip et al., 2018]. In real-world applications, known utility and probability weighting functions could originate from domain experts, surveys, or prior empirical studies on target user groups (see appendix F.6 for more details on the choice of the utility function) . In this work, we suppose that these are known. Our goal is to align the agent’s behavior with the given preferences by optimizing for the CPT value of returns. The known functions can be interpreted as the mathematical representation of the preferences that the agent must align with. Our main challenge consists in ensuring policy alignment with those predefined human preferences. We leave the question of discovering or inferring human preferences (e.g., inverse RL, RL from Human Feedback (RLHF)) which is central in many alignment problems to future work. See section E for an extended discussion comparing CPT-RL to RLHF as preference learning paradigms, their pros and cons and opportunities for future work in combining them as they are not mutually exclusive. We also refer the reader to appendix D for an extended discussion regarding applications.

Challenges. To conclude this section, we describe the challenges we face in solving (CPT-PO). First, the CPT value does not satisfy a Bellman equation due to the nonlinearity of the utility and weight functions which breaks the additivity and linearity of the standard expected return. Second, (CPT-PO) is a nonconvex problem involving several nonconvex functions: The utility itself is nonconvex in general (recall the utility is convex w.r.t. gains and concave w.r.t. losses) and the probabilities are also distorted by a nonconvex weight function. While the standard policy optimization problem is already nonconvex in the policy, (CPT-PO) further introduces additional nonconvexity.

3 About Optimal Policies in CPT-RL

In this section, we investigate the properties of optimal policies to (CPT-PO) when they exist. We focus on contrasting our results with existing known results for solving standard MDPs to highlight the peculiarities of our CPT-RL problem. Understanding the properties of optimal policies are important in view of designing efficient policy search algorithms.

We start our discussion by pointing out a stark difference between optimal policies in standard MDPs and (CPT-PO). While there exists an optimal *deterministic* stationary policy for MDPs (see e.g. Thm. 6.2.10 in Puterman [2014]), this is not the case in general for (CPT-PO).

Proposition 2. *There does not always exist an optimal policy for (CPT-PO) in Π_{NM}^D (i.e. deterministic non-Markovian).*

Proposition 2 tells us that the stochasticity of the policy is essential in solving our CPT-RL problem. The proof of this result is deferred to Appendix G.2: we construct a simple problem instance where an optimal policy needs to be stochastic as any deterministic policy is necessarily and clearly suboptimal. Our example is built around a w^+ function that puts special emphasis on the 10% of the best outcomes. As a consequence, the optimal policy needs to be randomized to take advantage of this and obtain the highest returns with some probability without suffering from bad outcomes by deterministically committing to this riskier strategy. It has been briefly mentioned in L.A. et al. [2016] that the policy needs to be random in general for (CPT-PO), see also the organ transplant example in Lin et al. [2018].

The next result shows that the need for stochasticity in the optimal policy is clearly due to the probability distortions in the CPT value. Indeed, when setting the probability weight distortion function w to the identity, i.e. when considering the particular case (EUT-PO) of (CPT-PO), it appears that an optimal policy is not necessarily stochastic.

Proposition 3. *There exists an optimal policy for (EUT-PO) in $\Pi_{\Sigma,NS}^D$.*

Proposition 3 allows to safely restrict our policy search to $\Pi_{\Sigma,NS}$ which is a much smaller policy space than the set of non-Markovian policies Π_{NM} . The fact that an optimal deterministic policy exists is a fundamental difference with the general (CPT-PO) setting. Whether there are specific weight functions (apart from the identity) for which there always exist a deterministic optimal policy remains an open question that we leave for future work.

Proposition 3 also shows that (EUT-PO) is simpler than the more general single-trial RL problem [Mutti et al., 2023a] in which one needs to look for an optimal policy in a much larger policy set Π_{NM}^D than $\Pi_{\Sigma,NS}^D$ in general. See appendix F.5 for the connection between both problems.

We now ask the next natural question: Can we further restrict our policy search to a smaller policy class compared to $\Pi_{\Sigma,NS}$? In particular, are there specific utility functions for which the resulting (EUT-PO) problem has optimal *Markovian* policies? We provide a positive answer by establishing a precise characterization of such utility functions which turn out to be either affine or exponential.

Theorem 4. *Let \mathcal{U} be continuous and increasing. The following statements are equivalent:*

1. *For any MDP, there exists an optimal policy for (EUT-PO) in $\Pi_{M,NS}$.*
2. *There exists $\varphi : \mathbb{R}^2 \rightarrow \mathbb{R}$ s.t. $\forall x, a, b \in \mathbb{R}, b \neq 0$,
 $\mathcal{U}(x+a) - \mathcal{U}(x) = \varphi(a, b)(\mathcal{U}(x+b) - \mathcal{U}(x))$.*
3. *There exists $\mu : \mathbb{R}^2 \rightarrow \mathbb{R}$ s.t. $\forall y, c, d \in \mathbb{R}$,
 $\mathcal{U}(y+c) - \mathcal{U}(c) = \mu(c, d)(\mathcal{U}(y+d) - \mathcal{U}(d))$.*
4. *There exist $A, B, C \in \mathbb{R}$ s.t. $\mathcal{U}(x) = Ax + B$ or $\mathcal{U}(x) = A + B \exp(Cx)$ for all $x \in \mathbb{R}$.*

A few comments are in order regarding Theorem 4:

(i) So far, we have highlighted the importance of the probability distortion function in determining the nature of optimal policies for (CPT-PO). Theorem 4 is rather concerned with the role of the (nonlinear) utility functions in (CPT-PO).

(ii) The theorem is reminiscent of the following known folklore result: The only memoryless continuous probability distribution is the exponential distribution.

(iii) Theorem 4 shows that the only utility functions leading to optimal *Markovian* policies are the affine and exponential utilities. The affine utility makes (CPT-PO) boil down to a standard RL problem whereas the exponential criterion is a well-known objective used in the risk-sensitive control and RL (see section 6 and appendix C for a discussion).

(iv) Monotonicity of the utility function is a fundamental assumption in economics and decision theory (utility increases with increasing gains). It is not crucial for most of our later developments though, see appendix F.7 for a discussion.

(v) Recall that our result holds for the finite horizon *undiscounted* setting which is not restrictive in applications. The discounted infinite horizon setting introduces additional technical challenges due to the lack of positive homogeneity of the CPT value, see Hau et al. [2023] (and Theorem 3.3 therein) for a discussion of this question for the particular case of the entropic risk measure. The use of positive quasi-homogeneity might allow to extend our result using similar techniques. We leave this for future work.

Theorem 4 is concerned with (EUT-PO) which is a particular case of (CPT-PO). However, these results cannot be extended to (CPT-PO) in general as we show next.

Proposition 5. *There exist instances of (CPT-PO) where \mathcal{U} is of the form $x \mapsto A + B \exp(Cx)$ for positive constants A, B, C and (CPT-PO) does not admit an optimal policy in $\Pi_{M,NS}$.*

4 Policy Gradient Algorithm for CPT-value Maximization

In this section, we propose a policy gradient algorithm for solving (CPT-PO). From this section on, we parametrize policies $\pi \in \Pi_{NM}$ by a vector $\theta \in \mathbb{R}^d$ and we denote by π_θ the parametrized policy. As a consequence, the CPT objective in (CPT-PO) becomes a function of the policy parameter θ and we use the shorthand notation $J(\theta)$ for the corresponding CPT objective value.

Our key result enabling our algorithm design is a PG theorem for CPT value maximization.

Theorem 6. (Policy Gradient for CPT-RL). *Suppose that the utility functions u^-, u^+ are continuous and that the weight functions w_-, w_+ are Lipschitz and differentiable. Assume in addition that the policy parametrization $\theta \mapsto \pi_\theta(a|h)$ (for any $h, a \in \mathcal{H} \times \mathcal{A}$) are both differentiable. Then, for every $\theta \in \mathbb{R}^d$, the gradient of the (CPT-PO) objective J w.r.t. the policy parameter θ is given by:*

$$\nabla J(\theta) = \mathbb{E} \left[\varphi(R(\tau)) \sum_{t=0}^{H-1} \nabla_\theta \log \pi_\theta(a_t|h_t) \right],$$

where $R(\tau) := \sum_{t=0}^{H-1} r_t$ with $\tau := (s_t, a_t, r_t)_{0 \leq t \leq H-1}$ is a trajectory of length H generated from the MDP by following policy π_θ^a and $\varphi(v) := \int_{z=0}^{\max(v,0)} w'_+(\mathbb{P}(u^+(R(\tau)) > z)) dz, - \int_{z=0}^{\max(-v,0)} w'_-(\mathbb{P}(u^-(R(\tau)) > z)) dz, \forall v \in \mathbb{R}$, and w'_+, w'_- denoting the derivatives.

^aThe integral $\varphi(R(\tau))$ is finite under our continuity assumptions since the return $R(\tau)$ is bounded.

We provide a few comments regarding this result. Theorem 6 recovers the celebrated policy gradient theorem for standard RL [Sutton et al., 1999] by setting w_+ (resp. w_-) to the identity function (on \mathbb{R}_+ (resp. \mathbb{R}^-) in which case w'_+ is the constant function equal to 1 and hence $\varphi(R(\tau)) = R(\tau)$). We stated the theorem in the general setting where the policy is non-Markovian. In practice, it is also possible to use a parametrization of a smaller policy set such as $\Pi_{\Sigma,NS}$ or even $\Pi_{M,S}$ in which the policy is a function of $(t, s_t, \sum_{k=0}^{t-1} r_k)$ or only s_t respectively.

Stochastic Policy Gradient Algorithm for CPT-RL. In the light of Theorem 6, we will perform a policy gradient ascent on the objective J to solve (CPT-PO). Our general policy gradient algorithm is presented in Algorithm 1. As usual, since we only have access to sampled trajectories from the MDP,

Algorithm 1 CPT-Policy Gradient Algorithm (CPT-PG)

- 1: **Input:** $\theta_0 \in \mathbb{R}^d$, utility functions u^+, u^- , weight functions w_+, w_- , step size $\alpha > 0$.
 - 2: **for** $k = 0, \dots, K$, **do**
 - /Policy gradient estimation
 - 3: Sample a trajectory $\tau := (s_t, a_t, r_t)_{0 \leq t \leq H-1}$, with $s_0 \sim \rho$ following π_{θ_k}
 - // Quantile estimation
 - 4: Sample n trajectories $\tau_j := (s_t^j, a_t^j, r_t^j)_{0 \leq t \leq H-1}$, $1 \leq j \leq n$ with $s_0^j \sim \rho$ following π_{θ_k}
 - 5: Compute and order $R(\tau_j)$, label them as $R(\tau_{[1]}) < R(\tau_{[2]}) < \dots < R(\tau_{[n]})$
 - 6: $\hat{\xi}_{\frac{i}{n}}^+ = u^+(R(\tau_{[i]}))$; $\hat{\xi}_{\frac{i}{n}}^- = u^-(R(\tau_{[i]}))$
 - //Approximation of $\varphi(R(\tau))$
 - 7: $\hat{\phi}_n^\pm = \sum_{i=0}^{j_n-1} w'_\pm \left(\frac{i}{n}\right) \left(\hat{\xi}_{\frac{n-i}{n}}^\pm - \hat{\xi}_{\frac{n-i-1}{n}}^\pm\right) + w'_\pm \left(\frac{j_n}{n}\right) \left(R(\tau) - \hat{\xi}_{\frac{n-j_n-1}{n}}^\pm\right)$
 - 8: $\hat{g}_k = (\hat{\phi}_n^+ - \hat{\phi}_n^-) \sum_{t=0}^{H-1} \nabla_\theta \log \pi_{\theta_k}(a_t | h_t)$
 - /Policy gradient update
 - 9: $\theta_{k+1} = \theta_k + \alpha \hat{g}_k$
 - 10: **end for**
-

we need a stochastic policy gradient to estimate the true unknown gradient given by the theorem. In particular, we need an approximation of $\varphi(R(\tau))$ for any sampled trajectory τ from the MDP following policy π_θ . In the case of (EUT-PO) in which w is the identity, the unknown quantity $\varphi(R(\tau))$ reduces to $\mathcal{U}(R(\tau))$ which can be easily computed as \mathcal{U} is known and $R(\tau)$ is the cumulative reward.

In the more general setting, the approximation task requires to compute the term $\int w'_+(\mathbb{P}(u^+(R(\tau)) > z) dz$ (and likewise for the second integral term). We address this challenge using the following result which is a variation of Proposition 6 in L.A. et al. [2016] in which the integrand is the derivative w'_+ (instead of w_+) and the integral is taken over a bounded interval. While L.A. et al. [2016] use this result to approximate the CPT value, we use it for approximating our special integral terms involving the derivatives of the weight functions as they appear in the policy gradient. We obtain a different approximation formula which is tailored to our setting. The approximation is essentially a Riemann sum using simple staircase functions.

Proposition 7. *Let X be a real-valued random variable. Suppose that the functions w'_+, w'_- are Lipschitz and that $u^+(X), u^-(X)$ have bounded first moments. Let $\xi_{\frac{i}{n}}^+$ and $\xi_{\frac{i}{n}}^-$ denote the $\frac{i}{n}$ th quantile of $u^+(X)$ and $u^-(X)$, respectively. Then, we have for any $v \geq 0$,*

$$\int_0^v w'_+(\mathbb{P}(u^+(X) > z)) dz = \lim_{n \rightarrow \infty} \sum_{i=0}^{j_n-1} w'_+ \left(\frac{i}{n}\right) \left(\hat{\xi}_{\frac{n-i}{n}}^+ - \hat{\xi}_{\frac{n-i-1}{n}}^+\right) + w'_+ \left(\frac{j_n}{n}\right) \left(v - \hat{\xi}_{\frac{n-j_n-1}{n}}^+\right), \quad (2)$$

where $j_n \in [0, n-1]$ is s.t. $v \in [\xi_{\frac{n-j_n-1}{n}}^+, \xi_{\frac{n-j_n}{n}}^+]$. The same identity holds when replacing $u^+(X), \xi_\alpha^+, w_+$ by $u^-(X), \xi_\alpha^-, w_-$ where ξ_α^- is the α^{th} quantile of $u^-(X)$.

Using Proposition 7, we approximate the integral using a finite sum with a given number of samples n . As for the quantiles $\xi_{\frac{i}{n}}^+$ we compute them using standard order statistics. Overall, compared to a vanilla PG algorithm, our additional required quantile estimation procedure requires a mild sorting step which can be executed in $\mathcal{O}(n \ln n)$ running time (without even invoking parallel implementations) where n is the length of the rewards to be sorted (see Algorithm 1).

Similarly to L.A. et al. [2016] (Theorem 1), our algorithm can be shown to enjoy a similar asymptotic convergence result to the set of stationary points of the (CPT-PO) objective. This is because we can also employ the same stochastic approximation artillery upon noticing that we are also approximating the same policy gradient differently and the induced bias in our case will also vanish with a large enough number of trajectories n (by Thm. 6 and Prop. 16). Notice that we can also remove the projection therein upon assuming that the rewards and the score function in the policy gradient are both bounded. These

fairly standard assumptions in the analysis of vanilla PG methods guarantee that the policy gradient will remain bounded.

Comparison to the CPT-SPSA-G algorithm in L.A. et al. [2016]. Our algorithm is specifically designed for maximizing the CPT value of a sum of rewards generated by an MDP while the CPT-SPSA-G algorithm in L.A. et al. [2016] can be used for a larger class of problems to maximize the CPT value of any real-valued random variable. However, we highlight that (a) this cumulative reward return structure is natural and ubiquitous in RL and economics applications and foremost (b) thanks to this particular problem structure, our algorithm is a policy gradient algorithm leveraging first-order information whereas CPT-SPSA-G only uses zeroth order information, i.e. CPT value estimations. This difference is crucial as zeroth order optimization algorithms are known to suffer from the curse of dimensionality. Our algorithm can scale better to higher dimensional problems as it is notoriously known for policy gradient algorithms in classic RL. We provide empirical evidence of this fact in section 5 to further support the benefits of our algorithm.

5 Simulations

We demonstrate the performance of our CPT-PG algorithm across three settings: (a) traffic control to show the influence of the probability distortion function, (b) scalability to larger state spaces compared to existing zeroth-order methods, and (c) continuous state-action space in an electricity management application. See appendix I and Table 2 for additional details and simulations in Appendix I.2-I.3 (theory illustrations), I.7 (financial trading) and I.8 (control).

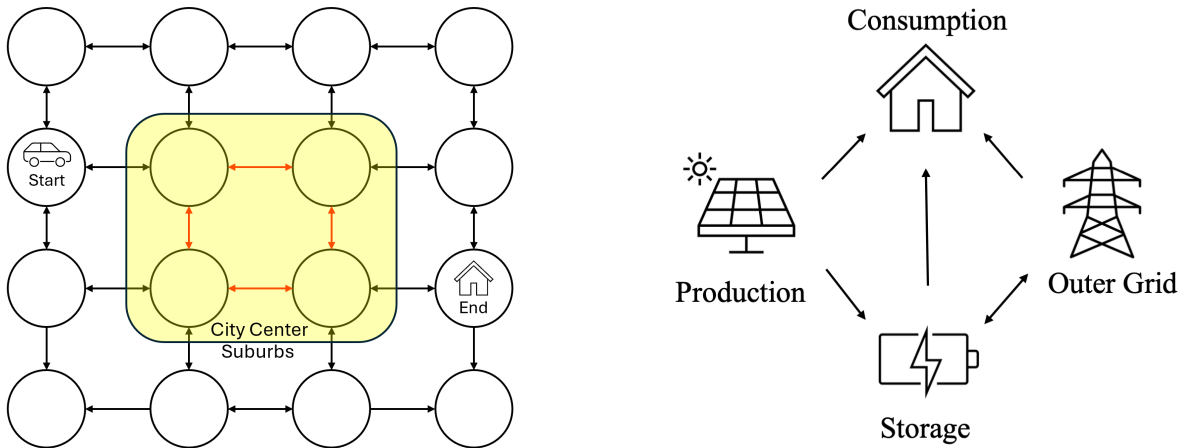


Figure 1: Environments: **(Left)** Traffic control: red roads in the city center are prone to congestion. **(Right)** Electricity management: arrows refer to electricity flow.

(a) Traffic control over a grid. We simulate a car agent navigating a city grid, where central roads are faster but risk higher delays (see fig. 1 center). The agent must balance speed against risk by avoiding the city center. In risk-neutral settings, the agent favors faster routes, while risk-averse policies avoid the risky central roads. Fig. 1 (center) demonstrates that our algorithm successfully adapts to different risk-weighted objectives. We also consider solving (CPT-PO) with different utility functions: risk-neutral identity utility, risk-averse KT utility, as well as exponential utility function. Fig. 2 show the corresponding different CPT returns observed. The obtained policies differ depending on the utility function. For examples of risk-neutral/averse policies obtained, see Fig. 19b in appendix I.4.

(b) Scalability to larger state spaces. We compare our PG algorithm with the zeroth-order (CPT-SPSA-G) of L.A. et al. [2016] on MDPs with increasing size $n \times n$. Fig. 3 highlights our algorithm’s scalability, while CPT-SPSA-G suffers with larger grids. See appendix I.4 for details.

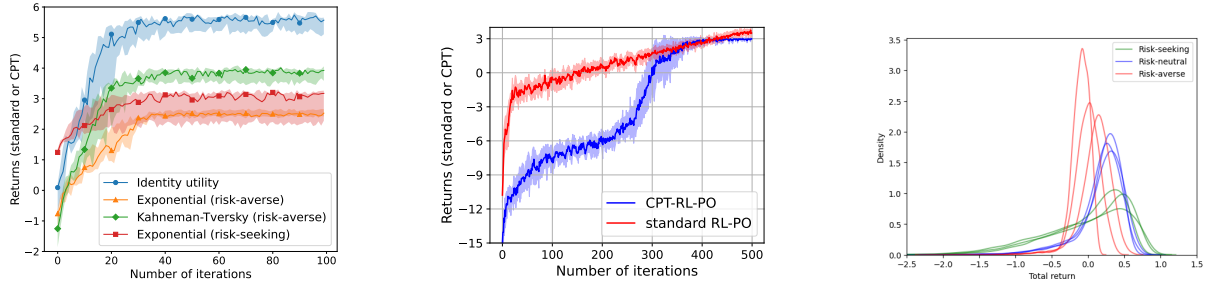


Figure 2: Returns along the iterations of our PG algorithm for (CPT-PO) for: (Left) different utility functions with the same distortion w in the grid environment, (Center) traffic control. Shaded areas indicate a range of \pm one standard deviation over 20 runs. (Right) Density of the empirical returns obtained by deploying different trained PG policies (from different initializations) for electricity management, density computed using 10,000 runs for each curve. See Appendix I for details.

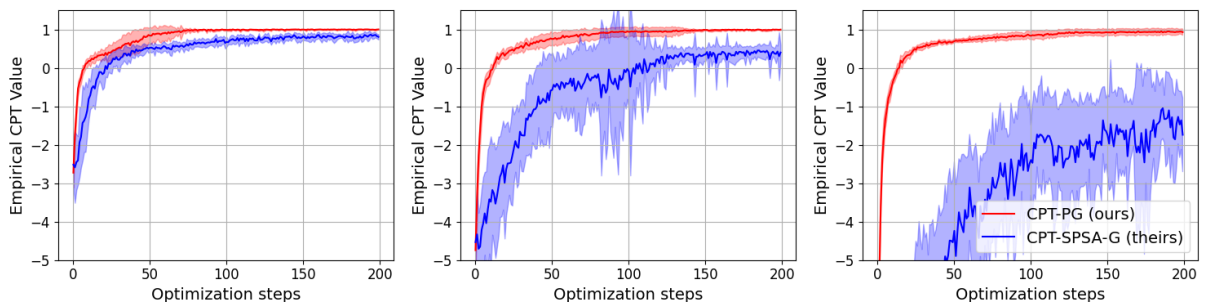


Figure 3: Compared performance of our algorithm and CPT-SPSA-G for $n = 3, 5, 9$. The shaded area is a range of \pm one standard deviation over 10 independent runs.

(c) **Electricity management.** In this application involving *continuous* state and action spaces, an individual home manages its electricity consumption and storage. We consider a 24-hour time frame where the agent must decide how much electricity to buy/sell, based on solar panel production, market prices, and battery levels. We use public data for selling prices recorded on a national electricity network. We experiment with risk-neutral, risk-averse, and risk-seeking objectives with 3 weight functions w . Our algorithm performs well across these scenarios, with the risk-averse policy minimizing downside risk, and the risk-seeking policy maximizing potential gains. Fig. (2) (right) shows the distribution of total returns for different objectives. The risk-averse policy avoids selling a lot of electricity and tends to keep it stored until the end of the day. Conversely, the risk-seeking policy aggressively sells energy when the markets are high at the cost of possibly having to buy it again later in the day. See appendix I.6 for more details.

6 Related Work

Prospect Theory and its sibling, CPT [Kahneman and Tversky, 1979, Tversky and Kahneman, 1992, Barberis, 2013], were first integrated with RL by L.A. et al. [2016]. Since then, only a few studies have explored the CPT-RL framework [Borkar and Chandak, 2021, Ramasubramanian et al., 2021, Ethayarajh et al., 2024]. Notably, Borkar and Chandak [2021] proposed a Q-learning algorithm for CPT-based policy optimization, while Ramasubramanian et al. [2021] developed value-based methods estimating CPT values using dynamic programming. Their approach optimizes a sum of CPT-transformed period costs, making it amenable to dynamic programming (see remark 1 therein). In contrast, our CPT formulation is different: we maximize the CPT value of the return of a policy (CPT-PO). This objective lacks an additive structure, hence does not satisfy a Bellman equation, rendering dynamic programming approaches inapplicable. Additionally, prior value-based methods are limited to finite state-action spaces, whereas our PG algorithm is also suitable for continuous state action settings, as shown in our experiments. More

recently, [Ethayarajh et al. \[2024\]](#) incorporated CPT (without probability distortion) for fine-tuning large language models with human feedback. Our work complements prior CPT-RL studies [[L.A. et al., 2016](#), [Jie et al., 2018](#)] that rely on zeroth-order SPSA methods [[Spall, 1992](#)]. Instead, we introduce a PG algorithm that leverages first-order information, exploiting the structure of CPT values applied to cumulative rewards (see [Section 4](#) for further comparison). Unlike existing PG approaches in risk-sensitive RL, our method explicitly accounts for probability distortion and S-shaped utility transformations, key aspects of CPT. For a broader discussion on CPT-RL, convex RL, and risk-sensitive RL, see [Appendix C](#). A diagram summarizing these connections is provided in [Appendix F.1](#).

7 Conclusion

We explored a CPT-based variant of RL to better model human decision-making, providing new insights into optimal policies and their differences from standard RL. We then introduced a novel PG algorithm for CPT-PO, demonstrating its scalability over prior methods and its effectiveness in simple applications. Our work opens several avenues for future research. CPT relies on predefined utility and distortion functions—can these be learned to better align with human preferences? Additionally, modeling collective human behavior through CPT in incentive design problems could be a promising direction. We hope this work inspires further research into capturing the complexity of human decision-making, beyond what expected utility theory alone can account for.

Acknowledgements

We thank the anonymous reviewers for their valuable comments that have helped improve this work.

References

- Q. Bai, M. Agarwal, and V. Aggarwal. Joint optimization of concave scalarized multi-objective reinforcement learning with policy gradient based algorithm. *Journal of Artificial Intelligence Research*, 74, Sept. 2022. 19
- A. Balbás, J. Garrido, and S. Mayoral. Properties of distortion risk measures. *Methodology and Computing in Applied Probability*, 11(3):385–399, 2009. 24
- A. Barakat, I. Fatkhullin, and N. He. Reinforcement learning with general utilities: Simpler variance reduction and large state-action space. In *Proceedings of the 40th International Conference on Machine Learning*, volume 202 of *Proceedings of Machine Learning Research*, pages 1753–1800. PMLR, 23–29 Jul 2023. 19
- A. Barakat, S. Chakraborty, P. Yu, P. Tokekar, and A. S. Bedi. Towards scalable general utility reinforcement learning: Occupancy approximation, sample complexity and global optimality. *arXiv preprint arXiv:2410.04108*, 2024. 19
- N. C. Barberis. Thirty years of prospect theory in economics: A review and assessment. *Journal of economic perspectives*, 27(1):173–196, 2013. 10, 19, 26
- M. G. Bellemare, W. Dabney, and M. Rowland. *Distributional reinforcement learning*. MIT Press, 2023. 19
- S. Bhatnagar, H. Prasad, and L. Prashanth. *Gradient Schemes with Simultaneous Perturbation Stochastic Approximation*, pages 41–76. Springer London, London, 2013. 19
- V. S. Borkar. Q-learning for risk-sensitive control. *Mathematics of operations research*, 27(2):294–311, 2002. 19
- V. S. Borkar and S. Chandak. Prospect-theoretic q-learning. *Systems & Control Letters*, 156:105009, 2021. 2, 10, 19

- Y. Chow and M. Ghavamzadeh. Algorithms for cvar optimization in mdps. *Advances in neural information processing systems*, 27, 2014. 19
- Y. Chow, M. Ghavamzadeh, L. Janson, and M. Pavone. Risk-constrained reinforcement learning with percentile risk criteria. *Journal of Machine Learning Research*, 18(167):1–51, 2018. 19
- D. Danis, P. Parmacek, D. Dunajsky, and B. Ramasubramanian. Multi-agent reinforcement learning with prospect theory. *2023 Proceedings of the Conference on Control and its Applications (CT)*, pages 9–16, 2023. 2, 20
- R. De Santi, M. Prajapat, and A. Krause. Global reinforcement learning : Beyond linear and convex rewards via submodular semi-gradient methods. In *Forty-first International Conference on Machine Learning*, 2024. 19
- S. Dorahaki, M. Rashidinejad, S. F. F. Ardestani, A. Abdollahi, and M. R. Salehizadeh. A home energy management model considering energy storage and smart flexible appliances: A modified time-driven prospect theory approach. *Journal of Energy Storage*, 48:104049, 2022. 2, 21, 27
- S. Ebrahimiagharehbaghi, Q. K. Qian, G. de Vries, and H. J. Visscher. Application of cumulative prospect theory in understanding energy retrofit decision: A study of homeowners in the netherlands. *Energy and Buildings*, 261:111958, 2022. 2, 20, 27
- K. Ethayarajh, W. Xu, N. Muennighoff, D. Jurafsky, and D. Kiela. Model alignment as prospect theoretic optimization. In *Forty-first International Conference on Machine Learning*, 2024. 10, 11, 19, 20, 23
- D. Gao, W. Xie, R. Cao, J. Weng, and E. W. M. Lee. The performance of cumulative prospect theory’s functional forms in decision-making behavior during building evacuation. *International Journal of Disaster Risk Reduction*, page 104132, 2023. 21, 27
- S. Gao, E. Frejinger, and M. Ben-Akiva. Adaptive route choices in risky traffic networks: A prospect theory approach. *Transportation research part C: emerging technologies*, 18(5):727–740, 2010. 21
- J. Garcia and F. Fernández. A comprehensive survey on safe reinforcement learning. *Journal of Machine Learning Research*, 16(1):1437–1480, 2015. 19
- M. Geist, J. Pérolat, M. Laurière, R. Elie, S. Perrin, O. Bachem, R. Munos, and O. Pietquin. Concave utility reinforcement learning: The mean-field game viewpoint. In *Proceedings of the 21st International Conference on Autonomous Agents and Multiagent Systems*, AAMAS ’22, page 489–497, 2022. 19
- S. A. George, J. Sheynin, R. Gonzalez, I. Liberzon, and J. L. Abelson. Diminished value discrimination in obsessive-compulsive disorder: A prospect theory model of decision-making under risk. *Frontiers in Psychiatry*, 10:469, 2019. 2, 5
- J. L. Hau, M. Petrik, and M. Ghavamzadeh. Entropic risk optimization in discounted mdps. In *International Conference on Artificial Intelligence and Statistics*, pages 47–76. PMLR, 2023. 7
- E. Hazan, S. Kakade, K. Singh, and A. Van Soest. Provably efficient maximum entropy exploration. In *International Conference on Machine Learning*, pages 2681–2691. PMLR, 2019. 19
- C. Jie, L. Prashanth, M. Fu, S. Marcus, and C. Szepesvári. Stochastic optimization in a cumulative prospect theory framework. *IEEE Transactions on Automatic Control*, 63(9):2867–2882, 2018. 11, 20
- D. Kahneman and A. Tversky. Prospect theory: An analysis of decision under risk. *Econometrica*, 47(2):263–291, 1979. 1, 3, 10, 19, 25
- P. L.A., C. Jie, M. Fu, S. Marcus, and C. Szepesvari. Cumulative prospect theory meets reinforcement learning: Prediction and control. In *Proceedings of The 33rd International Conference on Machine Learning*, volume 48 of *Proceedings of Machine Learning Research*, pages 1406–1415, New York, New York, USA, 20–22 Jun 2016. PMLR. 2, 6, 8, 9, 10, 11, 19, 20, 26
- R. Ladrón de Guevara Cortés, L. E. Tolosa, and M. P. Rojo. Prospect theory in the financial decision-making process: An empirical study of two argentine universities. *Journal of Economics, Finance and Administrative Science*, 28(55):116–133, 2023. 2, 21

- K. Lin, C. Jie, and S. I. Marcus. Probabilistically distorted risk-sensitive infinite-horizon dynamic programming. *Automatica*, 97:1–6, 2018. 6
- E. Luxenberg, P. Schiele, and S. Boyd. Portfolio optimization with cumulative prospect theory utility via convex optimization. *Computational Economics*, pages 1–21, 2024. 2, 22
- A. Mkrtchian, V. Valton, and J. P. Roiser. Reliability of decision-making and reinforcement learning computational parameters. *Computational Psychiatry*, 7(1):30, 2023. 2, 5
- M. Moharrami, Y. Murthy, A. Roy, and R. Srikant. A policy gradient algorithm for the risk-sensitive exponential cost mdp. *Mathematics of Operations Research*, 2024. 19
- M. Mutti, R. De Santi, and M. Restelli. The importance of non-markovianity in maximum state entropy exploration. In *Proceedings of the 39th International Conference on Machine Learning*, volume 162 of *Proceedings of Machine Learning Research*, pages 16223–16239. PMLR, 17–23 Jul 2022a. 19
- M. Mutti, R. D. Santi, P. D. Bartolomeis, and M. Restelli. Challenging common assumptions in convex reinforcement learning. *Advances in Neural Information Processing Systems*, 2022b. 19
- M. Mutti, R. De Santi, P. De Bartolomeis, and M. Restelli. Convex reinforcement learning in finite trials. *Journal of Machine Learning Research*, 24(250):1–42, 2023a. 6, 19
- M. Mutti, R. De Santi, P. De Bartolomeis, and M. Restelli. Convex reinforcement learning in finite trials. *Journal of Machine Learning Research*, 24(250):1–42, 2023b. 19, 26, 27
- E. Noorani, C. Mavridis, and J. Baras. Risk-sensitive reinforcement learning with exponential criteria. *arXiv preprint arXiv:2212.09010*, 2022. 19, 24
- L. Prashanth, M. C. Fu, et al. Risk-sensitive reinforcement learning via policy gradient search. *Foundations and Trends® in Machine Learning*, 15(5):537–693, 2022. 1, 19
- D. Prelec. The probability weighting function. *Econometrica*, 66(3):497–527, 1998. 3
- M. L. Puterman. *Markov decision processes: discrete stochastic dynamic programming*. John Wiley & Sons, 2014. 2, 6, 30, 31
- B. Ramasubramanian, L. Niu, A. Clark, and R. Poovendran. Reinforcement learning beyond expectation. In *2021 60th IEEE Conference on Decision and Control (CDC)*, pages 1528–1535, 2021. 2, 10, 19, 20, 26
- M. O. Rieger, M. Wang, and T. Hens. Estimating cumulative prospect theory parameters from an international survey. *Theory and Decision*, 82:567–596, 2017. 20, 23, 27
- U. Schmidt and H. Zank. What is loss aversion? *Journal of risk and uncertainty*, 30:157–167, 2005. 5
- E. N. Sereda, E. M. Bronshtein, S. T. Rachev, F. J. Fabozzi, W. Sun, and S. V. Stoyanov. Distortion risk measures in portfolio optimization. *Handbook of portfolio construction*, pages 649–673, 2010. 24
- K. E. Sip, R. Gonzalez, S. F. Taylor, and E. R. Stern. Increased loss aversion in unmedicated patients with obsessive-compulsive disorder. *Frontiers in Psychiatry*, 8:309, 2018. 2, 5
- J. C. Spall. Multivariate stochastic approximation using a simultaneous perturbation gradient approximation. *IEEE transactions on automatic control*, 37(3):332–341, 1992. 11, 20
- J. Sun, X. Zhou, J. Zhang, K. Xiang, X. Zhang, and L. Li. A cumulative prospect theory-based method for group medical emergency decision-making with interval uncertainty. *BMC Medical Informatics and Decision Making*, 22(1):124, 2022. 2
- R. S. Sutton, D. McAllester, S. Singh, and Y. Mansour. Policy gradient methods for reinforcement learning with function approximation. *Advances in neural information processing systems*, 12, 1999. 7
- A. Tamar, D. Di Castro, and S. Mannor. Policy gradients with variance related risk criteria. In *Proceedings of the twenty-ninth international conference on machine learning*, pages 387–396, 2012. 19

- E. Todorov, T. Erez, and Y. Tassa. Mujoco: A physics engine for model-based control. In *2012 IEEE/RSJ International Conference on Intelligent Robots and Systems*, pages 5026–5033. IEEE, 2012. doi: 10.1109/IROS.2012.6386109. 45, 46
- A. Tversky and D. Kahneman. Advances in prospect theory: Cumulative representation of uncertainty. *Journal of Risk and uncertainty*, 5:297–323, 1992. 1, 10, 19, 26
- N. Vijayan and P. LA. A policy gradient approach for optimization of smooth risk measures. In *The 39th Conference on Uncertainty in Artificial Intelligence*, 2023. 19
- J. L. Wirch and M. R. Hardy. Distortion risk measures: Coherence and stochastic dominance. In *International congress on insurance: Mathematics and economics*, pages 15–17, 2001. 25
- Q. Yan, T. Feng, and H. Timmermans. Investigating private parking space owners’ propensity to engage in shared parking schemes under conditions of uncertainty using a hybrid random-parameter logit-cumulative prospect theoretic model. *Transportation Research Part C: Emerging Technologies*, 120: 102776, 2020. 21, 27
- C. Yu, J. Liu, S. Nemati, and G. Yin. Reinforcement learning in healthcare: A survey. *ACM Computing Surveys (CSUR)*, 55(1):1–36, 2021. 4
- T. Zahavy, B. O’Donoghue, G. Desjardins, and S. Singh. Reward is enough for convex mdps. *Advances in Neural Information Processing Systems*, 34:25746–25759, 2021. 19
- J. Zhang, A. Koppel, A. S. Bedi, C. Szepesvari, and M. Wang. Variational policy gradient method for reinforcement learning with general utilities. *Advances in Neural Information Processing Systems*, 33: 4572–4583, 2020. 19
- J. Zhang, C. Ni, C. Szepesvari, and M. Wang. On the convergence and sample efficiency of variance-reduced policy gradient method. *Advances in Neural Information Processing Systems*, 34:2228–2240, 2021. 19
- M. Zhao, Y. Wang, X. Meng, and H. Liao. A three-way decision method based on cumulative prospect theory for the hierarchical diagnosis and treatment system of chronic diseases. *Applied Soft Computing*, 149:110960, 2023. 2

Contents

1	Introduction	1
2	From Classical RL to CPT-RL	2
3	About Optimal Policies in CPT-RL	5
4	Policy Gradient Algorithm for CPT-value Maximization	7
5	Simulations	9
6	Related Work	10
7	Conclusion	11
A	Notation for Policy Classes	16
B	CPT-RL vs Risk-Sensitive RL: An Illustration	17
C	Extended Related Work Discussion	19
	C.1 Risk-sensitive RL	19
	C.2 Convex RL/RL with General Utilities	19
	C.3 Cumulative Prospect Theoretic RL	19
D	Applications of CPT: From Prior Work in Stateless Settings to CPT-RL	20
	D.1 Energy: Renovation and Home Energy Management	20
	D.2 Security: Building Evacuation	21
	D.3 Urban Planning and Mobility	21
	D.4 Finance	21
	D.5 CPT-RL applications	22
E	CPT-RL and Trajectory-Based Reward RL as Preference Learning Paradigms	22
F	More about CPT Values and CPT Policy Optimization	23
	F.1 Positioning CPT-RL in the literature	23
	F.2 CPT value examples	24
	F.3 Proof: CVar, Var and distortion risk measures are CPT values	24
	F.4 Simple examples and further insights about CPT	25
	F.5 Connection to General Utility RL and Convex RL in finite trials	26
	F.6 Choice of the utility function	27
	F.7 Monotonicity assumption on the utility function	27
G	Proofs for Section 3	28
	G.1 Unwinding MDPs for CPT-RL	28
	G.2 Proof of Proposition 2	28
	G.3 Proof of Proposition 3	30
	G.4 Proof of Theorem 4	30
	G.5 Proof of Proposition 5	33
H	Proofs and Additional Details for Section 4	34
	H.1 Proof of Theorem 6	34
	H.2 Alternative Practical Procedure for Computing Stochastic Policy Gradients	35

I	More Details about Section 5 and Additional Experiments	37
I.1	Additional Figure	37
I.2	Illustration of Proposition 2: about the need for Stochastic Policies in CPT-RL	38
I.3	Illustration of Theorem 4: Markovian vs Non-Markovian Policies for CPT-RL	39
I.4	Grid Environment	40
I.5	Traffic Control	41
I.6	Electricity Management	41
I.7	Trading in Financial Markets	43
I.8	Control on MuJoCo Environments	45

A Notation for Policy Classes

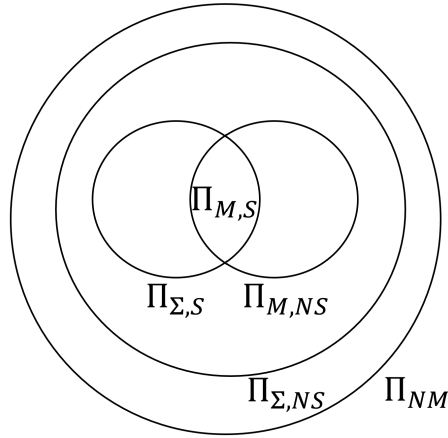


Figure 4: Policy classes (see Rem. 1).

Throughout this work, we will consider the following sets of policies:

- $\Pi_{NM} := \{\mathcal{H} \rightarrow \Delta(\mathcal{A})\}$ is the set of non-Markovian policies,³
- $\Pi_{\Sigma,NS} := \{\mathcal{S} \times \mathbb{R} \times \mathbb{N} \rightarrow \Delta(\mathcal{A})\}$ is the set of policies that only depend on the current state, the timestep and the sum of discounted rewards accumulated so far: The RL agent in state s at timestep t following policy $\pi \in \Pi_{\Sigma,NS}$ samples its next action from the distribution $\pi(s, \sum_{k=0}^{t-1} \gamma^k r_k, t)$,
- $\Pi_{\Sigma,S} := \{\mathcal{S} \times \mathbb{R} \rightarrow \Delta(\mathcal{A})\}$ is the set of policies that only depend on the state and the sum of discounted rewards: The RL agent in state s at timestep t following policy $\pi \in \Pi_{\Sigma,S}$ samples its next action from the distribution $\pi(s, \sum_{k=0}^{t-1} \gamma^k r_k)$,
- $\Pi_{M,NS} := \{\mathcal{S} \times \mathbb{N} \rightarrow \Delta(\mathcal{A})\}$ is the set of Markovian policies: An agent in state s at timestep t following policy $\pi \in \Pi_{M,NS}$ samples its next action from the distribution $\pi(s, t)$.
- $\Pi_{M,S} := \{\mathcal{S} \rightarrow \Delta(\mathcal{A})\}$ is the set of stationary Markovian policies, i.e. Markovian policies which are time-independent.

³By ‘non-Markovian’, we mean ‘*non necessarily* Markovian’ policies including Markovian ones. Elements of $\Pi_{NM} - \Pi_{M,NS}$ can be designated as ‘strictly non-Markovian’ policies. Likewise, by ‘non stationary’, we mean ‘non necessarily stationary’, and by ‘stochastic’ we mean ‘non necessarily deterministic’.

B CPT-RL vs Risk-Sensitive RL: An Illustration

In this section, we illustrate key features of CPT-RL compared to existing risk-sensitive RL approaches using a simple environment. This serves to provide intuition through an easy-to-grasp example. Specifically, we highlight how CPT-RL inflates low-probability (high-risk) events, distinguishing it from other methods. For comparison, we focus on an exponential risk-sensitive RL policy gradient algorithm, though similar results can also be shown for other risk-sensitive measures.

RiskyGridworld environment and reward structure. We consider a 5×5 custom gridworld environment. The agent starts at $(0, 0)$ and must navigate to the goal state $(4, 4)$, choosing between safe and risky paths.

- States: each cell represents a state. There are 3 risky states, two of which $((1,0), (2,2))$ correspond to penalty states and one is low probability high reward state (see reward description below), starting and goal states and the rest of the states are considered safe.
- Actions: The agent can move up, down, left, or right.
- Rewards: Safe steps incur a small penalty (-10) . The risky state $(2,4)$ offers a high reward (10^6) with low probability (0.01) , otherwise a large penalty (-10^3) . The remaining risky states give the same penalty. Reaching the goal provides a reward of $50,000$.
- Transitions: Movement is deterministic given the actions which are sampled according to the trained policy (which is not deterministic in our setting).

Algorithms for policy optimization. We compare our CPT-PG algorithm with an exponential risk-sensitive PG algorithm (using an exponential utility $(\mathcal{U}(x) = \frac{1}{\beta} \exp(-\beta x))$, $\beta = 0.1$, without probability weighting). For our CPT-PG algorithm, we use Kahneman and Tversky’s utility function with parameters $(x_0 = 1, \lambda = 3, \alpha = 0.6)$ (see section 2) and a probability weight function which is piecewise affine given by the following coefficients $w = [4, 0, 0.8, 0.2, 2.7, -1.7, 0.1, 0.9]$ where $[a_1, a_2, a_3, b_1, b_2, b_3, c_1, c_2]$ stands for a piecewise affine w function with $w(x) = a_i x + b_i$ for $c_{i-1} < x < c_i$. Note that this weight function inflates low probability events. This is one of the key features of CPT that we illustrate. We use a step size $\alpha = 0.01$ for both algorithms. For the policy network, we use a simple two-layer feed-forward neural network with a Leaky ReLU activation in the hidden layer and a softmax output layer for action selection.

Policy visualization. We provide heat maps visualizations of trained policy networks in the Risky-Gridworld environment, representing the probability of selecting a risky action at each state. For each state we define risky actions as the actions leading to risky states. Therefore, the only states possibly leading to risky states are the states adjacent to risky ones. For each one of these states we encode the risky action as the one leading to the risky state (choose the riskier one if there are multiple ones). Then the heatmap assigns to each state the probability of selecting the risky action associated to it (probability as provided by the trained policy under consideration in that state).

Results. See figures 5 and 6 and their captions in the next page.

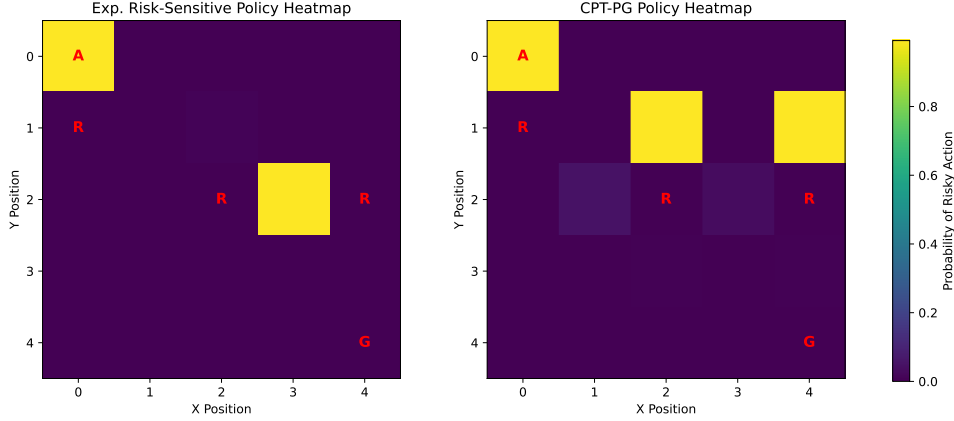


Figure 5: Heat maps representing the policies trained using our algorithm CPT-PG and an exponential risk-sensitive PG algorithm. Each cell in the 5×5 grid corresponds to a state, risky states are denoted by the letter ‘R’ in the cell, ‘A’ stands for the initial state and ‘G’ for the goal state, all the other states are considered safe (with a zero probability assigned). The color represents the probability of selecting a risky action at each state. The risky state (2,4) is risky in the sense that with low probability 0.01 it leads to high reward of 10^6 and a penalty of -10^3 otherwise. The main observation here is that CPT takes more risk in trying to end up in this risky state (low probability high reward) as you can see with the yellow cell above the risky state. Overall the risk profile is different for both methods. This is partly explained by the fact that CPT inflates low probability events thanks to the probability weight function.

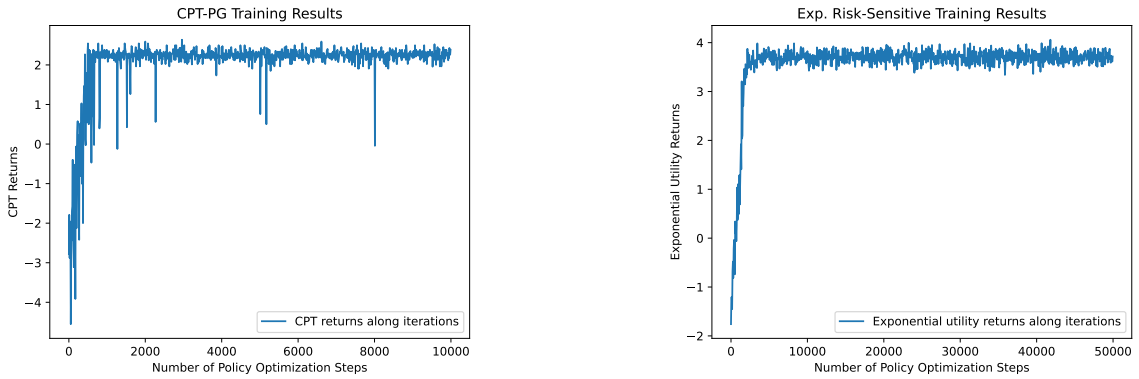


Figure 6: Policy training curves: **(Left)** CPT returns for CPT-PG. **(Right)** Exponential utility returns for Exponential Risk-Sensitive PG. Quantities are not comparable as one shows the CPT returns optimized in CPT policy optimization whereas the exponential risk-sensitive PG optimizes the exponential utility of the returns. Hence we represent them in separate graphs. This figure mainly serves the purpose of showing that the policies have been trained to maximize their respective objectives.

C Extended Related Work Discussion

C.1 Risk-sensitive RL

There is a rich literature around risk sensitive control and RL that we do not hope to give justice to here. We refer the reader to recent comprehensive surveys on the topic [Garcia and Fernández, 2015, Prashanth et al., 2022] and the references therein. Let us briefly mention that there exist several approaches to risk sensitive RL. These include formulations such as constrained stochastic optimization to control the tolerance to perturbations and stochastic minmax optimization to model robustness with respect to worst case perturbations for instance. Another approach which is more relevant to our paper discussion consists in regularizing or modifying objective functions. Such modifications are based on considering different statistics of the return deviating from the standard expectation such as the variance or the conditional value at risk (e.g. Tamar et al. [2012], Chow and Ghavamzadeh [2014], Chow et al. [2018]) or even considering the entire distribution of the returns like distributional RL [Bellemare et al., 2023]. Another popular objective modification consists in maximizing an exponential criterion (e.g. Borkar [2002], Noorani et al. [2022]) to obtain robust policies w.r.t noise and perturbations of system parameters or variations in the environment. Noorani et al. [2022] designed a model-free REINFORCE algorithm and an actor-critic variant of the algorithm leveraging an (approximate) multiplicative Bellman equation induced by the exponential objective criterion. Moharrami et al. [2024] recently proposed and analyzed similar PG algorithms for the same exponential objective. Vijayan and LA [2023] introduced a PG algorithm for solving risk-sensitive RL for a class of smooth risk measures including some distortion risk measures and a mean-variance risk measure. Their approach is based on simultaneous perturbation stochastic approximation (SPSA) [Bhatnagar et al., 2013] using zeroth-order information to estimate gradients. Our CPT-PO problem covers several of the aforementioned objectives including smooth distortion risk measures and exponential utility as particular cases (see appendix F for more details).

C.2 Convex RL/RL with General Utilities

In the last few years, convex RL (a.k.a. RL with general utilities) [Hazan et al., 2019, Zhang et al., 2020, Zahavy et al., 2021, Geist et al., 2022] has emerged as a framework to unify several problems of interest such as pure exploration, imitation learning or experiment design. More precisely, this line of research is concerned with maximizing a given functional of the state(-action) occupancy measure w.r.t. a policy. To solve this problem, several policy gradient algorithms have been proposed in the literature [Zhang et al., 2021, Bai et al., 2022, Barakat et al., 2023, 2024]. Mutti et al. [2022b,a, 2023a] challenged the initial problem formulation and proposed a finite trial version of the problem which is closer to practical concerns as it consists in maximizing a functional of the empirical state(-action) distribution rather than its true asymptotic counterpart. The particular case of our CPT policy optimization problem without probability distortion (see (EUT-PO) below) coincides with a particular case of the single trial convex RL problem [Mutti et al., 2023b] in which the function of the empirical visitation measure is a linear functional of the reward function (see appendix F.5 for details). However, our general problem is not a particular case of convex RL which does not account for probability distortions. Furthermore, our utility function is in general nonconvex in our setting (see example in Fig 8) and our policy gradient algorithm is model-free. More recently, De Santi et al. [2024] introduced a *global* RL problem formulation where rewards are globally defined over trajectories instead of locally over states and used submodular optimization tools to solve the resulting non-additive policy optimization problem. While global RL allows to account for trajectory-level global rewards, it does not take into consideration probability distortions. In addition, their investigation is restricted to the setting where the transition model is known whereas our PG algorithm is model-free.

C.3 Cumulative Prospect Theoretic RL

Motivated by Prospect Theory and its sibling CPT [Kahneman and Tversky, 1979, Tversky and Kahneman, 1992, Barberis, 2013], L.A. et al. [2016] first proposed to combine CPT with RL to obtain a better model for human decision making. Following this first research effort, only few isolated works [Borkar and Chandak, 2021, Ramasubramanian et al., 2021, Ethayarajh et al., 2024] considered a similar CPT-RL setting. In particular, Borkar and Chandak [2021] proposed and analyzed a Q-learning algorithm for

CPT policy optimization. [Ramasubramanian et al. \[2021\]](#) further developed value-based algorithms for CPT-RL by estimating the CPT value of an action in a given state via dynamic programming. More precisely, they were concerned with maximizing a sum of CPT value period costs which is amenable to dynamic programming. In contrast to their accumulated CPT-based cost (see their remark 1), our CPT policy optimization problem formulation is different: we maximize the CPT value of the return of a policy (see (CPT-PO)). In particular, this objective does not enjoy an additive structure and hence does not satisfy a Bellman equation. Moreover, their work relying on value-based methods is restricted to finite discrete state action spaces. Our PG algorithm is also suitable for continuous state action settings as we demonstrate in our experiments. More recently, [Ethayarajh et al. \[2024\]](#) incorporated CPT (without probability distortion) into RL from human feedback for fine-tuning large language models. CPT has also been recently exploited for multi-agent RL [[Danis et al., 2023](#)]. Our work is complementary to this line of research, especially to [L.A. et al. \[2016\]](#) and its extended version [Jie et al. \[2018\]](#) which are the most closely related work to ours. While their algorithm design makes use of simultaneous perturbation stochastic approximation (SPSA) [[Spall, 1992](#)] using only zeroth order information, we rather propose a PG algorithm exploiting first-order information thanks to our special problem structure involving the CPT value of a cumulative sum of rewards. See section 4 for further details regarding this comparison.

We refer the reader to Appendix F.1 for a summarizing diagram illustrating the relationships between CPT-RL, convex RL and risk-sensitive RL.

D Applications of CPT: From Prior Work in Stateless Settings to CPT-RL

In this section, we provide a discussion regarding the applications where CPT has already been successfully used (mainly in the static stateless setting) and potential applications in the dynamic (RL) setting with state transitions.

We highlight that CPT has been tested and effectively used in a large number of compelling behavioral studies that we cannot hope to give justice to here. Besides the initial findings of Tversky and Kahneman for which the latter won the Nobel Prize in economics in 2002, please see a few recent references below for a broad spectrum of real-world applications ranging from economics to transport, security and energy, mostly in the stateless (static) setting.

- Risk preferences across 53 countries worldwide in an international survey [[Rieger et al., 2017](#)]. Estimates of CPT parameters from data illustrate economic and cultural differences whereas probability weighting also reflects gender differences as well as economic and cultural impacts. Note here the explainability feature of CPT.

‘We conduct a standardized survey on risk preferences in 53 countries worldwide and estimate cumulative prospect theory parameters from the data. The parameter estimates show that significant differences on the cross-country level are to some extent robust and related to economic and cultural differences. In particular, a closer look on probability weighting underlines gender differences, economic effects, and cultural impact on probability weighting.’

D.1 Energy: Renovation and Home Energy Management

- A study of homeowners in the Netherlands to investigate energy retrofit decision using CPT [[Ebrahimigharehbaghi et al., 2022](#)]. CPT is shown to predict the number of homeowners decisions to renovate their homes more accurately than Expected Utility Theory (EUT).

‘CPT correctly predicts the decisions of 86 % of homeowners to renovate their homes to be energy efficient or not. EUT, on the other hand, overestimates the number of decisions to renovate: it incorrectly predicts retrofit for 52 % of homeowners who did not renovate for energy efficiency reasons. Using the estimated parameters of CPT, the cognitive biases of reference dependence, loss aversion, diminishing sensitivity, and probability weighting can be clearly seen for different target groups.’

- Home energy management [Dorahaki et al., 2022]. This work proposes a behavioral home energy management model to increase the user’s satisfaction.

‘Smart home is a small but an important energy segment that has a significant potential to implement authentic energy policies, where human is a major decision-maker in the home energy management dilemma. Therefore, humans’ emotions and tendencies plays a vital role as the End-User’s daily decisions. In this paper, we develop a behavioral home energy management model based on time-driven prospect theory incorporating energy storage devices, distributed energy resources, and smart flexible home appliances. [...] The results of the simulation studies show that the End-User’s satisfaction in the proposed home energy management behavioral structure will be increased substantially compared with the conventional monetary home energy management models.’

D.2 Security: Building Evacuation

- Application of CPT to building evacuation [Gao et al., 2023]. CPT allows to take into account individual psychology and irrational behavior in modeling evacuations via pedestrian movement modeling. This is particularly important for designing and optimizing emergency and safety management strategies.

‘Understanding the performance of decision-making behavior in building evacuation is essential for predicting pedestrian dynamics, designing appropriate facility safety management, optimizing emergency management strategies, and reducing the impact of disasters. While many pedestrian movement models have been developed based on the hypothesis of rational and strategic decision-making, only a limited number of works consider individual psychology and irrational behavior. To address this issue, we have successfully integrated the cumulative prospect theory (CPT) into modeling evacuations.’

D.3 Urban Planning and Mobility

- **Parking:** Understanding private parking space owners’ propensity to share their parking spaces by considering their psychological concerns as well as their socio-demographic and revenue characteristics for instance [Yan et al., 2020]. This might be useful to help developing shared parking services.

‘Results show that socio-demographic characteristics, context variables, revenues and psychological concerns are all important factors in explaining parking space owners’ propensity to engage in platform-based shared parking schemes. [...] Understanding parking space owners’ propensity to share their parking spaces in relation to their psychological concerns and uncertain conditions is critical to improve shared parking policies. The results of this paper may help designers and planners in the delivery of shared parking services and promote the success and future growth of the shared parking industry.’

- **Traffic routing.** Gao et al. [2010] model the travelers’ strategic behavior for route choice in a stochastic network when adapting to traffic conditions which are revealed en route.

D.4 Finance

- Empirical study about financial decision making in two universities in Argentina [Ladrón de Guevara Cortés et al., 2023]. In particular, it is shown that the financial decisions of the participants under uncertainty are more consistent with Prospect Theory than expected utility theory.

‘This paper aims to provide empirical evidence for using the prospect theory (PT) basic assumptions in the Argentine context. Mainly, this study analysed the financial decision-making process in students of the economic-administrative academic area of two universities, one public and one private, in Córdoba. [...] The empirical results provided evidence on the effects of certainty, reflection and isolation in both universities, concluding that the study participants make financial decisions in situations of uncertainty based more on PT than on expected utility theory. This study contributes to the empirical evidence in a different

Latin-American context, confirming that individuals make financial decisions based on the PT [...].’

D.5 CPT-RL applications

Our CPT-RL problem formulation finds applications in a number of diverse areas. A nonexhaustive list includes:

- **Traffic control.** We refer the reader to our toy example in the main part. simulations for specific CPT-RL applications in simple settings for traffic control, electricity management and financial trading that we will not discuss again here.
- **Electricity management.** Please see simulations in the main part (section 5 and appendix I.6) in a simple example setting to illustrate our methodology.
- **Finance:** portfolio optimization, risk management, behavioral asset pricing (e.g. influence of investor sentiment on price dynamics via e.g. over-weighting of low-probability events, including their preferences). For recent applications of CPT to finance, we refer the reader to a recent paper [Luxenberg et al. \[2024\]](#) using CPT for portfolio optimization (in a stateless static setting). We also applied our methodology to financial trading (see Appendix I.7).
- **Health:** personalized treatment plans, (e.g. health insurance design for specific groups modeling risk and factoring perceived fairness).

On a more high-level note, we would like to mention that CPT-RL is of practical relevance for finance and healthcare for several reasons: in short, CPT allows for (a) **modeling human biases**, (b) **factoring risk**, and (c) **capturing individual preferences for personalization**. All these three points are essential in the above applications.

Many other meaningful human-centric applications are yet to be explored, including: such as

- **Legal and ethical decision making,**
- **Cybersecurity,**
- **Human-robot interaction,**
- ...

E CPT-RL and Trajectory-Based Reward RL as Preference Learning Paradigms

In this section, we compare the CPT-RL and trajectory-based reward RL (using a single reward for the entire trajectory, such as Reinforcement Learning from Human Feedback) seen as preference learning paradigms. In particular, we also discuss the pros and cons of each one of them.

Regarding the structure of the final reward and the metric learning you mention, this is a fair point and we agree that Our present work requires so far access to utility and weight functions whereas trajectory-based reward RL learns the metric to be optimized using human preference data. However, let us mention a few points:

- (a) These can be readily available in specific applications (for risk modeling or even chosen at will by the users themselves);
- (b) CPT relies on a predefined model, this can be beneficial in applications such as portfolio optimization or medical treatment where trade-offs have to be made and models might be readily available;
- (c) Furthermore, we argue that having such a model allows it to be more explainable compared to a model entirely relying on human feedback and fine tuning, let alone the discussion about the cost of collecting human feedback. We also note that some of the most widely used algorithms in RLHF (e.g. DPO) do rely on the fact that the reward follows a Bradley-Terry model for instance (either for learning the reward or at least to derive the algorithm to bypass reward learning);

- (d) Let us mention that one can also learn the utility and weight functions. We mentioned this promising possibility in our conclusion although we did not pursue this direction in this work. One can for instance represent the utility and weight functions by neural networks and train models to learn them using available data with relevant losses, jointly with the policy optimization task. One can also simply fit the predefined functions (say e.g. Tversky and Kahneman’s function) to the data by estimating the parameters of these functions (see η with our notations and exponents of the utility function in Table 1 for the CPT row). This last approach is already commonly used in practice, see e.g. Rieger et al. [2017].

CPT vs RLHF: General comparison. CPT has been particularly useful when modeling specific biases in decision making under risk to account for biased probability perceptions. It allows to *explicitly* model cognitive biases. In contrast, RLHF has been successful in training LLMs which are aligned with human preferences where these are complex and potentially evolving and where biases cannot be explicitly and reasonably modeled. RLHF has been rather focused on learning *implicit* human preferences through interaction (e.g. using rankings and/or pairwise comparisons). Overall, CPT can be useful for tasks where risk modeling is essential and critical whereas RLHF can be useful for general preference alignment although RLHF can also be adapted to model risk if human preferences are observable and abundantly available at a reasonable cost. This might not be the case in healthcare applications for instance, where one can be satisfied with a tunable risk model. On the other hand, so far CPT does not have this ability to adapt to evolving preferences over time unlike RLHF which can do so via feedback.

CPT and RLHF: Pros and cons. To summarize the pros and cons of both approaches, we provide the following elements. As for the pros, CPT directly models psychological human biases in decision making via a structured framework which is particularly effective for risk preferences. RLHF can generalize to different scenarios with sufficient feedback and handle complex preferences via learning from diverse human interactions, it is particularly useful in settings where preferences are not explicitly defined such as for LLMs for aligning the systems with human preferences and values. As for the cons, CPT is a static framework since the utility and probability weight functions are fixed, it is hence less adaptive to changing preferences. It uses a predefined model of human behavior which is not directly using feedback. It also requires to estimate model parameters precisely, often for specific domains. As for RLHF on the other hand, the quality and the quantity of the human feedback is essential and this dependence on the feedback clearly impacts performance. This dependence can also cause undesirable bias amplification which is present in the human feedback. We also note that training such models is computationally expensive in large scale applications.

CPT and RLHF are not mutually exclusive. While CPT and trajectory-based RL (say e.g. RLHF) both offer frameworks for incorporating human preferences into decision making, we would like to highlight that CPT and RLHF are not mutually exclusive. We can for instance use CPT to design an initial reward structure reflecting human biases, then refine it with RLHF. We can also consider to further relax the requirement of sum of rewards (which already has several applications on its own) and think about incorporating CPT features to RLHF. Some recent efforts in the literature in this direction that we mentioned in our paper include the work of Ethayarajh et al. [2024] which combines prospect theory with RLHF (without probability weight distortion though, which limits its power). Note that the ideas of utility transformation and probability weighting are not crucially dependent on the sum of rewards structure and can also be applied to trajectory-based rewards or trajectory frequencies for instance. We believe this direction deserves further research, one interesting point would be how to incorporate risk awareness from human behavior to such RLHF models using ideas from CPT.

F More about CPT Values and CPT Policy Optimization

F.1 Positioning CPT-RL in the literature

Remark 8. For the infinite horizon discounted setting, the objective becomes the CPT value of the random variable $X = \sum_{t=0}^{+\infty} \gamma^t r_t$ recording the cumulative discounted rewards induced by the MDP and the policy π . The policy can further be parameterized by a vector parameter $\theta \in \mathbb{R}^d$.

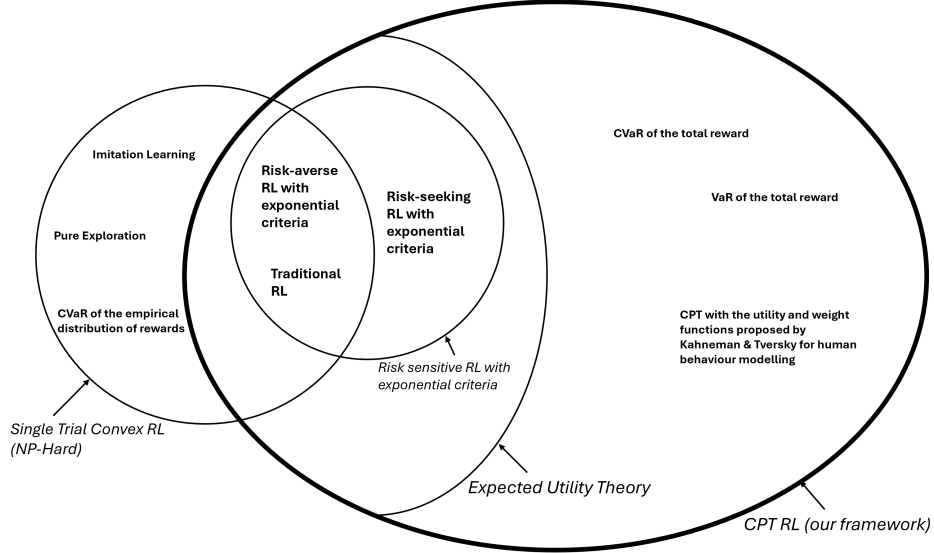


Figure 7: A Venn Diagram representing our framework and some other frameworks in the literature

F.2 CPT value examples

Setting	Utility function	w^+	w^-
CPT	Any	Any	Any
CPT (Functions proposed by Kahneman and Tversky)	$\begin{cases} (x - x_0)^\alpha & \text{if } x \geq 0, \\ -\lambda(x - x_0)^\alpha & \text{if } x < 0 \end{cases}$	$\frac{p^\eta}{(p^\eta + (1-p)^\eta)^{\frac{1}{\eta}}}$	$\frac{p^\delta}{(p^\delta + (1-p)^\delta)^{\frac{1}{\delta}}}$
EUT	Any	Identity function	Identity function
Distortion risk measure	Identity function	Any	$1 - w^+(1 - t)$
CVaR* (Balbás et al. [2009])	Identity function	$1 - w^-(1 - t)$	$\begin{cases} \frac{x}{1-\alpha} & \text{if } 0 \leq x < 1 - \alpha, \\ 1 & \text{if } 1 - \alpha \leq x \leq 1 \end{cases}$
VaR* [Balbás et al., 2009]	Identity function	$1 - w^-(1 - t)$	$\begin{cases} 0 & \text{if } 0 \leq x < 1 - \alpha, \\ 1 & \text{if } 1 - \alpha \leq x \leq 1 \end{cases}$
Risk-sensitive RL with exponential criteria [Noorani et al., 2022]	$\frac{1}{\beta} \exp(\beta x), \beta > 0$	Identity function	Identity function

Table 1: CPT value examples. *: Note that w^+ and w^- are discontinuous for VaR and CVaR.

F.3 Proof: CVar, Var and distortion risk measures are CPT values

For a random variable X and a non-decreasing function $g : [0, 1] \rightarrow [0, 1]$ with $g(0) = 0$ and $g(1) = 1$, the **distortion risk measure** [Sereda et al., 2010] is defined as:

$$\rho_g(X) := \int_{-\infty}^0 \tilde{g}(F_{-X}(x)) dx - \int_0^{+\infty} g(1 - F_{-X}(x)) dx,$$

where $F_{-X} : t \mapsto \mathbb{P}(-X \leq t)$ and $\tilde{g} : t \mapsto 1 - g(1 - t)$.

Proposition 9. Any distortion risk measure of a given random variable X can be written as a CPT value with $u^+ = id^+$, $u^- = -id^-$, $w^+ = \tilde{g}$ and $w^- = g$.

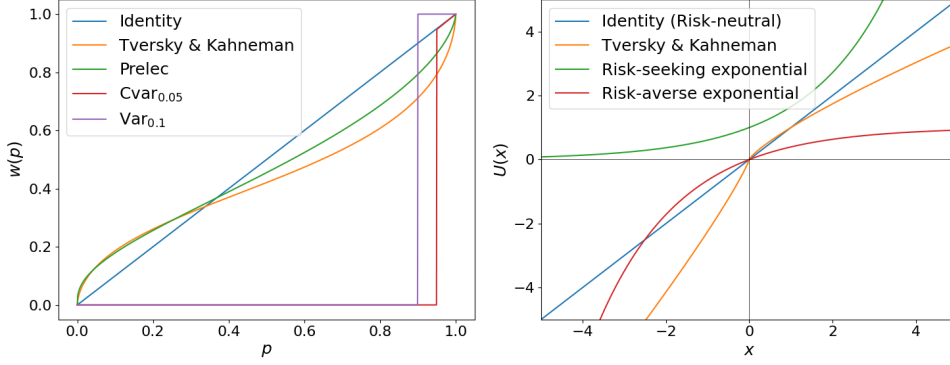


Figure 8: Various examples of probability weight functions (left) and utility functions (right).

Proof. It follows from the definition of the distortion risk measure together with a simple change of variable $x \mapsto -x$ that:

$$\begin{aligned}
\rho_g(X) &= \int_{-\infty}^0 \tilde{g}(F_{-X}(x))dx - \int_0^{+\infty} g(1 - F_{-X}(x))dx \\
&= - \int_{+\infty}^0 \tilde{g}(F_{-X}(-x))dx - \int_0^{+\infty} g(1 - F_{-X}(x))dx \\
&= \int_0^{+\infty} \tilde{g}(F_{-X}(-x))dx - \int_0^{+\infty} g(1 - F_{-X}(x))dx \\
&= \int_0^{+\infty} \tilde{g}(\mathbb{P}(-X \leq -x))dx - \int_0^{+\infty} g(1 - \mathbb{P}(-X \leq x))dx \\
&= \int_0^{+\infty} \tilde{g}(\mathbb{P}(X \geq x))dx - \int_0^{+\infty} g(\mathbb{P}(-X > x))dx.
\end{aligned}$$

Since $g(\mathbb{P}(-X > x)) = g(\mathbb{P}(-X \geq x))$ almost everywhere (in a measure theoretic sense) on $[0, +\infty[$, and g is bounded, we obtain:

$$\rho_g(X) = \int_0^{+\infty} \tilde{g}(\mathbb{P}(X \geq x))dx - \int_0^{+\infty} g(\mathbb{P}(-X \geq x))dx.$$

We recognize the CPT-value of X with $u^+ = \text{id}^+$, $u^- = -\text{id}^-$, $w^+ = \tilde{g}$ and $w^- = g$. \square

Remark 10. When X admits a density function, Value at Risk (VaR) and Conditional Value at Risk (CVaR) (Wirch and Hardy [2001]) have been shown to be special cases of distortion risk measures and are therefore also instances of CPT-values.

F.4 Simple examples and further insights about CPT

Human decision makers might not act rationally due to psychological biases and personal preferences, their decisions might not necessarily be dictated by expected utility theory. Consider this simple example as a first illustration: A player must choose between (A) receiving a payoff of 80 and (B) participating in a lottery and receive either 0 or 200 with equal probability. The player's preference depends on their attitude towards risk. While a risk-neutral agent will be satisfied with the immediate and safe payoff of 80, another individual might want to try to obtain the much higher 200 payoff. In particular, different agents might perceive the same utility and the same random outcome differently. Furthermore, they can exhibit both risk-seeking and risk-averse behaviors depending on the context.

Therefore, due to its failure to capture such settings as a descriptive model, the standard expected utility theory has been called into question by the pioneering behavioral psychologist Daniel Kahneman together with his colleague Amos Tversky [Kahneman and Tversky, 1979]. In particular, Daniel Kahneman has been awarded the Nobel Prize in Economic Sciences in 2002 "for having integrated insights from

psychological research into economic science, especially concerning human judgment and decision-making under uncertainty”. In their seminal works combining cognitive psychology and economics, they laid the foundations of the so-called prospect theory and its cumulative version later on [Tversky and Kahneman, 1992] to explain several empirical observations invalidating the standard expected utility theory.

Let us illustrate this in a simple example borrowed from Ramasubramanian et al. [2021] (example 2 in section IV therein) for the purpose of our exposition. Consider a game where one can either earn \$100 with probability (w.p.) 1 or earn 10000 w.p. 0.01 and nothing otherwise. A human might rather lean towards the first option which gives a certain gain. In contrast, if the situation is flipped, i.e., a loss of 100 w.p. 1 versus a loss of \$10000 w.p. 0.01, then humans might rather choose the latter option. In both settings, the expected gain or loss has the same value (100). The CPT paradigm allows to model the tendency of humans to perceive gains and losses differently. Moreover, the humans tend to deflate high probabilities and inflate low probabilities [Tversky and Kahneman, 1992, Barberis, 2013]. For instance, as exposed in L.A. et al. [2016], humans might rather choose a large reward, say 1 million dollars w.p. 10^{-6} over a reward of 1 w.p. 1 and the opposite when rewards are replaced by losses.

F.5 Connection to General Utility RL and Convex RL in finite trials

In this section, we elaborate in more details on one of the connections we noticed (and mentioned in related works) between our (CPT-PO) problem of interest and the literature of generality utility RL.

First, we recall a few notations complementing the preliminaries. Any fixed policy π and any initial state distribution ρ induce together a state occupancy measure d_ρ^π recording the visitation frequency of each state, it is defined at each state $s \in \mathcal{S}$ by $d_\rho^\pi(s) := \sum_{t=0}^{H-1} \mathbb{P}_{\rho, \pi}(s_t = s)$. The corresponding state-action occupancy measure is defined for every state-action pair $(s, a) \in \mathcal{S} \times \mathcal{A}$ by $\mu_\rho^\pi(s, a) := d_\rho^\pi(s)\pi(a|s)$. Recall that $J(\pi) = \langle \mu_\rho^\pi, r \rangle := \sum_{s \in \mathcal{S}, a \in \mathcal{A}} \mu_\rho^\pi(s, a)r(s, a)$ for any policy π and any initial state distribution ρ .

The general utility RL problem consists in maximizing a (non-linear in general) functional of the occupancy measure induced by a policy. More formally, the general utility RL can be written as follows:

$$\max_{\pi} F(d_\rho^\pi), \quad (3)$$

where F is the real valued utility function defined on the set of probability measures over the state or state-action space, ρ is the initial state distribution and d_ρ^π is the state (or sometimes state-action) occupancy measure induced by the policy π . This problem captures the standard RL problem as a particular case by considering a linear functional F defined using a fixed given reward function. Recently, motivated by practical concerns, Mutti et al. [2023b] argued for the relevance of a variation of the problem under the qualification of *convex RL in finite trials*. They introduce for this the empirical state distributions $d_n \in \Delta(\mathcal{S})$ defined for every state $s \in \mathcal{S}$ by:

$$d_n^\pi(s) = \frac{1}{nT} \sum_{i=1}^n \sum_{t=0}^{T-1} \mathbb{1}(s_{t,i} = s), \quad (4)$$

where $s_{t,i}$ is the state at time t resulting from the interaction with the MDP (with policy π) in the i -th episode, among n independent trials. Their policy optimization problem is then as follows:

$$\max_{\pi} \xi_n(\pi) := \mathbb{E}[F(d_n^\pi)]. \quad (5)$$

Note that d_n^π is a random variable as it is an empirical state distribution. Observe also that $\lim_{n \rightarrow \infty} \xi_n(\pi) = F(d_\rho^\pi)$ under mild technical conditions (e.g. continuity and boundedness of F). This shows the connection between the above final trial convex RL objective and the general utility RL problem (3). The interesting differences between both problem formulations arise for small values of n . Of particular interest, both in this paper and in Mutti et al. [2023b], is the *single trial RL* setting where $n = 1$.

Setting the probability distortion function w to be the identity, our (CPT-PO) problem becomes (EUT-PO), i.e.:

$$\max_{\pi} \mathbb{E} \left[\mathcal{U} \left(\sum_{t=0}^{H-1} r_t \right) \right], \quad (6)$$

which is of the form $\xi_1(\pi)$, the single-trial RL objective as defined in Mutti et al. [2023b]. Indeed, it suffices to write the following to observe it:

$$\mathcal{U}\left(\sum_{t=0}^{H-1} r_t\right) = \mathcal{U}(\langle d_1^\pi, r \rangle), \quad (7)$$

where r is the reward function seen as a vector in $\mathbb{R}^{|\mathcal{S}|}$, $\langle \cdot, \cdot \rangle$ is the standard Euclidean product in $\mathbb{R}^{|\mathcal{S}|}$. Therefore, it appears that the above objective is indeed a functional of the empirical distribution d_1^π . Single trial general utility RL is more general than (EUT-PO) since it does not necessarily consider an additive reward inside the non-linear utility and can accommodate any (convex) functional of the occupancy measure. However, (CPT-PO) does not appear to be a particular case of single trial convex RL because of the probability distortion function introduced.

F.6 Choice of the utility function

We provide here additional comments regarding the choice of the utility function to complement our brief discussion in the main part of the paper. The problems themselves might dictate to the user or decision maker the utility function to be used. The user might also design their own according to their own beliefs, behaviors and objectives, based on the goal to be achieved (e.g. risk-seeking, risk-neutral, risk-averse). Specific applications might also suggest specific utility functions such as specific risk measures like in risk sensitive RL for instance. We have provided in table 1 a list of different examples one might consider. Learning the utility function is also an interesting direction to investigate as we mention in the conclusion. In practice, it is rather common to use the example we provide in table 1 (CPT row) with exponent parameters which are estimated using data. We provide a few concrete examples in the following. For instance, Rieger et al. [2017] adopt such an approach (see sections 3.1, 3.2 and 3.3 therein for a detailed discussion about parameter estimation). Ebrahimigharehbaghi et al. [2022] choose some similar variation of this utility (see eqs. 2-3 therein) while still using KT’s probability weighting functions. Gao et al. [2023] compare different functions for different similar power utility functions with fitted parameters (see Tables 1, 2 and 3 therein p. 3, 4, 6 for extensive comparisons with the existing literature). Similar investigations were conducted in Yan et al. [2020]. Dorahaki et al. [2022] consider psychological time discounted utility functions (variations of the same power functions) in their model with additional relevant hyperparameters, motivated by (domain-specific) psychological studies (see eq. (4) therein). It is worth noting that all these examples are only in the static stateless setting.

F.7 Monotonicity assumption on the utility function

We provide a few comments about the monotonicity assumption we make in Theorem 4 for instance, and its implications for the remaining results of the paper. We argue below that this is not a restriction and it is not fundamentally needed for our algorithm:

- We focus on the monotone setting because typical human behavior tends to prefer better outcomes over worst ones, e.g. higher gains over smaller ones and smaller losses over larger losses. This is captured by the monotonicity assumption on the utility function: utility increases with increasing gains and decreases with increasing losses. This is a fundamental assumption in economics and decision theory which is consistent with how humans evaluate outcomes. Nevertheless, there are certainly cases where this assumption might not hold.
- Strict monotonicity is needed in some of the proofs of our results, mainly Theorem 4, see e.g. proof of (1) implies (2) and proof of (5) implies (2). However, it is not formally required to derive our policy gradient theorem. Note also that even Proposition 7 for estimating the integrals does not require it as soon as denote the right quantiles as we defined them in the proposition. See point 3 below for further comments.
- Mere monotonicity is mainly useful in our algorithm to guarantee that the utility values are sorted in the same order as the returns obtained from the sampled trajectories (see quantile estimation computation step of the algorithm). This leads to a simple computation of the quantiles of the utilities: Once the returns are sorted, the utilities are also sorted in the same way and quantiles can be read from the

sorted list. If monotonicity does not hold anymore, one has to be more careful about this computation and adapt the step of the algorithm accordingly by simply computing the quantiles of the utilities using the right sorting of these (which would be different from the sorting of the returns). In that case, sorting the returns is not needed and one only needs to sort the utilities (utility function applied to the returns). Apart from this technical detail, we do not foresee any major impediment to using the algorithm without the strict monotonicity assumption.

G Proofs for Section 3

G.1 Unwinding MDPs for CPT-RL

In this section, we describe an equivalent MDP construction that will be used in some of our proofs such as for Proposition 3. For any CPT-MDP $(\mathcal{S}, \mathcal{A}, r, P)$ with utility function \mathcal{U} , we can formally define an equivalent ‘unwinded’ MDP⁴ that can be solved using classical RL techniques. For any state $s \in \mathcal{S}$ is the original MDP and any timestep $t \leq H - 1$ with cumulative reward $\sum_{k=0}^t r_k$, we associate a state $\tilde{s} := (s, t, \sum_{k=0}^t r_k)$ and the rewards in the unwinded MDP are adjusted as to reflect the difference in utility between two consecutive states:

$$\tilde{r}_t = \mathcal{U} \left(\sum_{k=1}^{t+1} r_k \right) - \mathcal{U} \left(\sum_{k=1}^t r_k \right). \quad (8)$$

We observe that all the information needed at any given timestep to take a decision on the next action to take is contained in \tilde{s} . This implies that any CPT-value that can be achieved by a non-Markovian strategy on the original MDP can also be achieved by a Markovian policy on the unwinded MDP.

The reader might notice that the size of the unwinded MDP grows with the horizon length and might blow up depending on the original MDP structure. As a consequence, learning in this unwinded MDP might become intractable. If the original MDP can be represented as a finite directed acyclic graph, the unwinded MDP is also a finite directed acyclic graph. If the underlying MDP contains a cycle, even if it is finite, its unwinded version may contain an infinite number of states. In the case of a stochastic tree MDP, the unwinded MDP has the exact same shape as the original one.

Note that we will only be using the unwinded MDP as a theoretical construction to prove some of our results and we do not perform any learning task in this unwinded MDP.

G.2 Proof of Proposition 2

To prove the proposition, we consider a simple MDP with only two states (an initial state and a terminal one) and two actions (A and B). See Fig. 14a below. We choose the identity as utility. Action A yields reward 1 with probability 1 and action B yields either 0 or $\frac{3}{2}$ with probability $\frac{1}{2}$ each. We further consider the following probability distortion function $w^+ : [0, 1] \rightarrow [0, 1]$ defined for every $x \in [0, 1]$ as follows:

$$w^+(x) = \begin{cases} 5x & \text{if } x \leq 0.1, \\ \frac{1}{2} + \frac{5}{9}(x - 0.1) & \text{otherwise,} \end{cases} \quad (9)$$

and we set $w^- = 0$. All the policies can be described with a single scalar $p \in [0, 1]$, the probability of choosing B instead of A.

The CPT value of the reward X is:

$$\mathbb{C}(X) = w^+ \left(1 - \frac{p}{2} \right) + \frac{1}{2} w^+ \left(\frac{p}{2} \right). \quad (10)$$

There are only two possible deterministic policies:

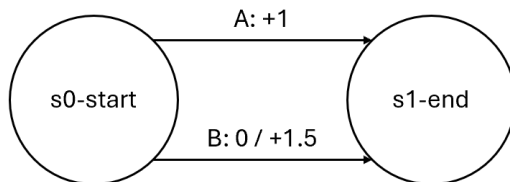
- For the policy corresponding to $p = 0$, $\mathbb{C}(X) = 1$.
- For the policy corresponding to $p = 1$, $\mathbb{C}(X) = \frac{3}{2} w^+ \left(\frac{1}{2} \right) = \frac{13}{12} \approx 1.08$.

⁴This terminology is not standard, we adopt it here to describe our approach.

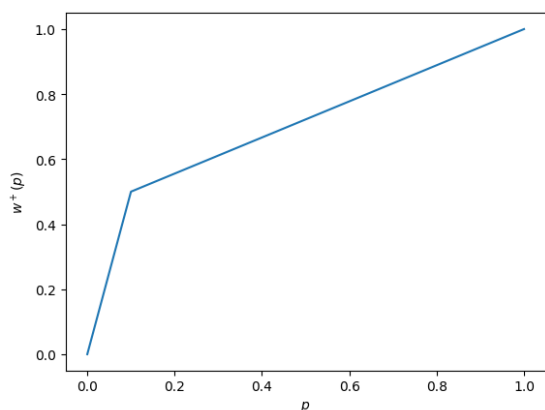
However, with the non-deterministic policy $p = 0.2$, we get:

$$\mathbb{C}(X) = w^+(0.9) + \frac{1}{2}w^+(0.1) = \frac{17}{18} + \frac{1}{4} = \frac{43}{36} \approx 1.19$$

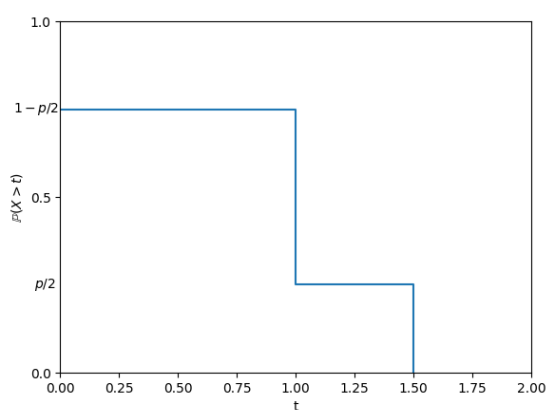
which is larger than the CPT values of both deterministic policies. We conclude that there are no deterministic policies solving the CPT problem in this case.



(a) The MDP



(b) The w^+ function



(c) The $t \mapsto \mathbb{P}(X > t)$ function

Figure 9: Problem instance for the proof of Proposition 2.

Remark 11. We provided a counterexample with random rewards, but there also exist counterexamples with deterministic rewards. One way to build such a counterexample is to start from the MDP we just studied and ‘transfer’ the randomness from the reward functions to the probability transition, by constructing a larger -but equivalent- MDP, with intermediate states like in Fig. 10.

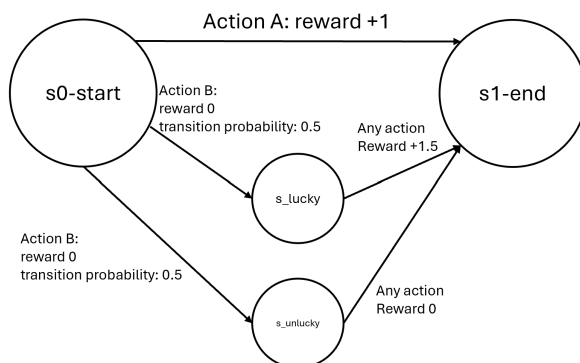


Figure 10: An equivalent example with deterministic rewards

G.3 Proof of Proposition 3

We build a classical MDP which is equivalent to our CPT-MDP following the procedure described in more details in appendix G.1. In summary, we expand every state s in our CPT MDP into several states encoding the state, partial sum of rewards and timestep all at once, i.e. $\tilde{s} = (s, t, \sum_{k=0}^{t-1} r_k)$. We encode all the dynamics of our CPT MDP into our new conventional MDP, and the reward in our new MDP when going from a state $\tilde{s}_a = (s_a, \sigma_a, t_a)$ to another state $\tilde{s}_b = (s_b, \sigma_b, t_a + 1)$ is simply defined as $\mathcal{U}(\sigma_b) - \mathcal{U}(\sigma_a)$. We see that any non-Markovian policy in the CPT MDP can be rewritten as a non-Markovian policy in the new classical MDP and reciprocally, any non-Markovian policy in the new, classical MDP can be rewritten as a non-Markovian policy in the original CPT MDP. Moreover, choosing 1 as a discounting factor in the new MDP, we note that by telescoping sum, the total reward in the new MDP corresponds exactly to the total utility of the sum of rewards in the CPT MDP. Since it is a classical MDP, our new MDP admits a Markovian optimal policy [Puterman, 2014]. This optimal policy is at least as good as any other non-Markovian policy in the new MDP with regards to the expected total reward and therefore at least as good as any other non-Markovian policy in the old CPT MDP with regards to *expected utility* of the total reward. When translating this optimal policy to a policy in the CPT MDP, we notice it only depends on $(s, \sum_{k=0}^{t-1} r_k, t)$, meaning it is indeed an element of $\Pi_{\Sigma, NS}$. This concludes the proof.

G.4 Proof of Theorem 4

We will prove the following extended version of Theorem 4.

Theorem 12. *Let \mathcal{U} be continuous and (strictly) increasing. The following statements are equivalent:*

1. For any MDP, there exists an optimal policy for (EUT-PO) in $\Pi_{M, NS}$.
2. There exists a function $\varphi : \mathbb{R}^2 \rightarrow \mathbb{R}$ such that:

$$\forall x, a, b \in \mathbb{R}, b \neq 0, \mathcal{U}(x+a) - \mathcal{U}(x) = \varphi(a, b)(\mathcal{U}(x+b) - \mathcal{U}(x)).$$

3. There exists $\alpha \in \mathbb{R}$ s.t. $\mathcal{U}''(x) = \alpha \mathcal{U}'(x)$ for all $x \in \mathbb{R}$.
4. There exist $A, B, C \in \mathbb{R}$ s.t. $\mathcal{U}(x) = Ax + B$ or $\mathcal{U}(x) = A + B \exp(Cx)$ for all $x \in \mathbb{R}$.
5. There exists a function $\mu : \mathbb{R}^2 \rightarrow \mathbb{R}$ such that:

$$\forall y, c, d \in \mathbb{R}, \mathcal{U}(y+c) - \mathcal{U}(c) = \mu(c, d)(\mathcal{U}(y+d) - \mathcal{U}(d)).$$

We prove a series of implications and equivalences. It can be easily verified from combining all these results that $1 \implies 2 \implies 3 \implies 4 \implies 5 \implies 1$, which proves all the equivalences of the theorem. We proceed to prove each one of our implications in the rest of this section.

Proof of $3 \Leftrightarrow 4$, $4 \Rightarrow 2$, and $4 \Rightarrow 5$. The equivalence $3 \Leftrightarrow 4$ is obtained simply by solving the differential equation for one implication and a simple calculation for the other implication. The implications $4 \Rightarrow 2$ and $4 \Rightarrow 5$ follow from simple algebraic verification.

Proof of $5 \Rightarrow 2$.

We suppose 5 holds. For any given $a, b \in \mathbb{R}$ such that $b \neq 0$, we define $\varphi(a, b) := \frac{\mathcal{U}(1+a) - \mathcal{U}(1)}{\mathcal{U}(1+b) - \mathcal{U}(1)}$. Notice that this quantity is well defined since \mathcal{U} being (strictly) increasing (and $b \neq 0$) implies that $\mathcal{U}(1+b) - \mathcal{U}(1) \neq 0$. Then, we use 5 to obtain that for every $x \in \mathbb{R}$,

$$\mathcal{U}(x+b) - \mathcal{U}(x) = \mu(x, 1)(\mathcal{U}(1+b) - \mathcal{U}(1)). \quad (11)$$

We conclude the proof of the implication by writing:

$$\begin{aligned} \mathcal{U}(x+a) - \mathcal{U}(x) &= \mu(x, 1)(\mathcal{U}(1+a) - \mathcal{U}(1)) && \text{(again by 5)} \\ &= \varphi(a, b)\mu(x, 1)(\mathcal{U}(1+b) - \mathcal{U}(1)) && \text{(using the above definition of } \varphi(a, b)) \\ &= \varphi(a, b)(\mathcal{U}(x+b) - \mathcal{U}(x)). && \text{(using Eq. (11))} \end{aligned}$$

This shows that 2 holds and concludes the proof.

Proof of 2 \Rightarrow 4. Consider a fixed integer k . Let $C_k := \varphi(2 \cdot 2^{-k}, 2^{-k})$ and $u_n := \mathcal{U}(n2^{-k})$ for every $n \in \mathbb{N}$. We have the following recurrence relation for all $n \in \mathbb{N}$:

$$u_{n+2} - u_n = C_k(u_{n+1} - u_n).$$

That is to say for every $n \in \mathbb{N}$,

$$u_{n+2} - C_k u_{n+1} + (C_k - 1)u_n = 0.$$

This recurrence relation can be solved by examining the characteristic polynomial:

$$x^2 - C_k x + (C_k - 1) = 0.$$

The roots are obtained using the quadratic formula: $r_{\pm} = \frac{C_k \pm \sqrt{C_k^2 - 4(C_k - 1)}}{2} = \frac{C_k \pm (C_k - 2)}{2}$.

- If $C_k = 2$, there is only one root, 1, and $\exists D_k, E_k \in \mathbb{R}, \forall n, u_n = (D_k n + E_k)1^n = D_k n + E_k$
- Otherwise, there are two real roots, $(C_k - 1)$ and 1, and u_n is of the form, $u_n = D_k(C_k - 1)^n + E_k \cdot 1^n = D_k C_k^n + E_k$.

This proves that for all k , there exists a function in $\{x \mapsto Ax + b, (A, B) \in \mathbb{R}^2\} \cup \{x \mapsto A + B \exp(Cx), (A, B) \in \mathbb{R}^2\}$ that coincides with \mathcal{U} on the set $\{\frac{x}{2^k}, x \in \mathbb{N}\}$.

Importantly, all these functions have to be the same (across different values of k , i.e. all D_k constants are the same and all E_k constants do also coincide), due to the structure of $\{x \mapsto Ax + b, (A, B) \in \mathbb{R}^2\} \cup \{x \mapsto A + B \exp(Cx), (A, B) \in \mathbb{R}^2\}$ and because they all coincide on all the integers with the corresponding value of the same (fixed) utility function \mathcal{U} at the relevant integer. This means that there exists a single function f in $\{x \mapsto Ax + b, (A, B) \in \mathbb{R}^2\} \cup \{x \mapsto A + B \exp(Cx), (A, B) \in \mathbb{R}^2\}$ which coincides with \mathcal{U} on all of $\{\frac{x}{2^y}, x \in \mathbb{N}, y \in \mathbb{N}^+\}$. By continuity of \mathcal{U} , we obtain that 4 holds.

Proof of 4 \Rightarrow 1.

If \mathcal{U} is an affine function $x \mapsto Ax + B$ (for some $A, B \in \mathbb{R}$), then solving the (EUT-PO) problem boils down to solving a traditional MDP in which an optimal Markovian policy always exists [Puterman, 2014].

Let us now assume that the utility function is of the form $x \mapsto A + B \exp(Cx)$ for some $A, B, C \in \mathbb{R}$. Without loss of generality, we can simply ignore the constant A in the optimization problem (EUT-PO) and just assume we are maximizing $\mathcal{U}(x) = B \exp(Cx)$. Recall that we are considering a finite-horizon setting with horizon length H . For any $0 \leq T \leq H$, we say that a policy $\pi \in \Pi_{\Sigma, NS}$ is **Markovian in the last T steps** if there exists a function f defined from $\mathcal{S} \times \mathbb{N}$ (into the set of policies) such that:

$$\forall \sigma \in \mathbb{R}, \forall t \geq H - T, \forall s \in \mathcal{S}, \pi(s, \sigma, t) = f(s, t).$$

Using again the unwinded MDP construction like in the proof of Proposition 3, we can find a policy $\pi^* \in \Pi_{\Sigma, NS}^D$ which is "totally" optimal: that is to say, starting from any (s, σ, t) , $\mathbb{E} \left[\mathcal{U}(\sigma + \sum_{k=t}^{H-1} r_k) \right]$ is maximal when following policy π^* . We proceed by induction to prove the assertion \mathcal{P}_T : 'There exists a deterministic totally optimal policy π_T which is Markovian in the last T steps' for any $T \leq H$, especially for $T = H$ which is the desired result.

Initialization: \mathcal{P}_0 is true with $\pi_0 = \pi^*$.

Induction: Let us suppose \mathcal{P}_T is true for some $T < H$. We define π_{T+1} by:

$$\pi_{T+1}(s, \sigma, t) := \begin{cases} \pi_T(s, 0, t) & \text{if } t = H - T - 1 \\ \pi_T(s, \sigma, t) & \text{otherwise.} \end{cases}$$

We see that π_{T+1} is a deterministic policy that is Markovian in the last $T + 1$ steps. We also see that for any $t \geq H - T$ and any $\sigma \in \mathbb{R}, s \in \mathcal{S}$, starting from (s, σ, t) , $\mathbb{E} \left[\mathcal{U}(\sigma + \sum_{k=t}^{H-1} r_k) \right]$ is maximal when following policy π_{T+1} . We need to prove it for others values of t . i.e. $t \leq H - T - 1$.

Because π_{T+1} is Markovian in the last $T + 1$ steps, the probability distribution on future states, actions and rewards starting from $(s, \sigma, H - T - 1)$ does not depend on σ .

We know that it optimizes $\mathbb{E} \left[\mathcal{U}(0 + \sum_{k=t}^{H-1} r_k) \right]$, and we want to show that it optimizes $\mathbb{E} \left[\mathcal{U}(\sigma + \sum_{k=H-T-1}^{H-1} r_k) \right]$ for all $\sigma \in \mathbb{R}$. This is where we use the form of the utility function to remark that

$$\mathbb{E} \left[\mathcal{U} \left(\sigma + \sum_{k=H-T-1}^{H-1} r_k \right) \right] = \mathbb{E} \left[\exp(C\sigma) \mathcal{U} \left(\sum_{k=H-T-1}^{H-1} r_k \right) \right] = \exp(C\sigma) \mathbb{E} \left[\mathcal{U} \left(\sum_{k=H-T-1}^{H-1} r_k \right) \right]$$

and a maximizer for $\sigma = 0$ is therefore a maximizer for all σ .

We know now that π_{T+1} is optimal starting from any (s, σ, t) if $t \geq H - T - 1$. Note that now, step $H - T - 1$ is included.

Starting from (s, σ, t) with $t < H - T - 1$, we know that π_T maximizes $\mathbb{E} \left[\mathcal{U}(\sigma + \sum_{k=t}^{H-1} r_k) \right]$. We notice, using the tower rule:

$$\begin{aligned} \mathbb{E} \left[\mathcal{U} \left(\sigma + \sum_{k=t}^{H-1} r_k \right) \right] &= \mathbb{E} \left[\mathcal{U} \left(\sigma + \sum_{k=t}^{H-T-2} r_k + \sum_{k=H-T-1}^{H-1} r_k \right) \right] \\ &= \mathbb{E} \left[\mathbb{E} \left[\mathcal{U} \left(\underbrace{\sigma + \sum_{k=t}^{H-T-2} r_k}_{\sigma'} + \sum_{k=H-T-1}^{H-1} r_k \mid \underbrace{\sigma + \sum_{k=t}^{H-T-2} r_k, s_{H-T-1}}_{\sigma'} \right) \right] \right]. \end{aligned}$$

Because π_{T+1} is as good as π_T at maximizing $\mathbb{E} \left[\mathcal{U} \left(\sigma' + \sum_{k=H-T-1}^{H-1} r_k \right) \right]$ starting from $(\sigma', s_{H-T-1}, T - H - 1)$, we conclude that π_{T+1} performs as well as π_T , because the inner conditional expectation is the same and the first steps are the same.

Therefore, \mathcal{P}_{T+1} is true.

Conclusion: \mathcal{P}_H is true, which is our desired result.

Proof of 1 \Rightarrow 2.

Let us show $-2 \Rightarrow -1$. -2 means that for any function $\varphi : \mathbb{R}^2 \mapsto \mathbb{R}$, there exists $x, a, b \in \mathbb{R}$ such that $b \neq 0$ and $\mathcal{U}(x + a) - \mathcal{U}(x) \neq \varphi(a, b)(\mathcal{U}(x + b) - \mathcal{U}(x))$.

Define now $\varphi : \mathbb{R}^2 \mapsto \mathbb{R}$ by $\varphi(\alpha, \beta) = \frac{\mathcal{U}(\alpha) - \mathcal{U}(0)}{\mathcal{U}(\beta) - \mathcal{U}(0)}$ for all $\alpha \in \mathbb{R}, \beta \neq 0$ and $\varphi(\alpha, \beta) = 1$ for $\beta = 0$. It follows that there exist $x, a \in \mathbb{R}, b \neq 0$ (given by -2 above) such that $\mathcal{U}(x + a) - \mathcal{U}(x) \neq \varphi(a, b)(\mathcal{U}(x + b) - \mathcal{U}(x))$.

As a consequence, we obtain $\frac{\mathcal{U}(x+a) - \mathcal{U}(x)}{\mathcal{U}(x+b) - \mathcal{U}(x)} \neq \frac{\mathcal{U}(a) - \mathcal{U}(0)}{\mathcal{U}(b) - \mathcal{U}(0)}$. Our idea now is to exploit this difference in utility to build a situation in which a non-Markovian strategy is clearly more profitable in view of our (EUT-PO) policy optimization problem.

Suppose without loss of generality that $b > a > 0$ and $\frac{\mathcal{U}(x+a) - \mathcal{U}(x)}{\mathcal{U}(x+b) - \mathcal{U}(x)} > \frac{\mathcal{U}(a) - \mathcal{U}(0)}{\mathcal{U}(b) - \mathcal{U}(0)}$ without loss of generality. In the other cases, the inequalities might get reversed but the gist of the proof stays the same. We define p as the halfpoint

$$p := \frac{1}{2} \left(\frac{\mathcal{U}(x+a) - \mathcal{U}(x)}{\mathcal{U}(x+b) - \mathcal{U}(x)} + \frac{\mathcal{U}(a) - \mathcal{U}(0)}{\mathcal{U}(b) - \mathcal{U}(0)} \right). \quad (12)$$

Since \mathcal{U} is strictly increasing, we have that $p \in (0, 1)$.

We now consider an MDP with three states s_0, s_1, s_2 where s_2 is a terminal state that leads to nowhere and s_0 is the starting state. Whatever action is taken in s_0 , we transition to s_1 , with reward x with probability $\frac{1}{2}$ and reward y with probability $\frac{1}{2}$. Once in state s_1 , we can take action A, which yields reward a with probability 1, or take action B, which yields reward b with probability p and 0 otherwise. Both lead to s_2 and the end of the episode with certainty. Here, to maximize the (EUT-PO) objective, one has to adopt a non-Markovian strategy in s_1 , hence disproving assertion 1. Indeed, knowing the reward achieved in the past step (between states s_0 and s_1) allows to decide whether to take more risks or not to achieve a higher EUT return.

We elaborate on this claim in what follows. Observe first that

$$\frac{\mathcal{U}(x+a) - \mathcal{U}(x)}{\mathcal{U}(x+b) - \mathcal{U}(x)} > p > \frac{\mathcal{U}(a) - \mathcal{U}(0)}{\mathcal{U}(b) - \mathcal{U}(0)}. \quad (13)$$

What is the best action to choose if we are in state s_1 and have had return 0 so far? We know there is a deterministic best action to take. Action 1 yields total reward $\mathcal{U}(a)$. Choosing action 2 yields:

$$\mathbb{E}(\mathcal{U}(r_0 + r_1)|r_0 = 0) = \mathbb{E}(\mathcal{U}(r_1)) = p\mathcal{U}(b) + (1-p)\mathcal{U}(0) = p(\mathcal{U}(b) - \mathcal{U}(0)) + \mathcal{U}(0) > \mathcal{U}(a), \quad (14)$$

where the strict inequality follows from using (13). So it is *strictly* better to choose action 2 over action 1 if we are in s_1 and have had a return 0 so far.

What is the best action to choose if we are in state s_1 and have had return x so far? We know again that there is a deterministic best action to take. Action 1 yields total reward $\mathcal{U}(x+a)$. Choosing action 2 yields:

$$\begin{aligned} \mathbb{E}(\mathcal{U}(r_0 + r_1)|r_0 = x) &= \mathbb{E}(\mathcal{U}(r_1 + x)) = p\mathcal{U}(b+x) + (1-p)\mathcal{U}(x) \\ &= p(\mathcal{U}(b+x) - \mathcal{U}(x)) + \mathcal{U}(x) < \mathcal{U}(a+x), \end{aligned} \quad (15)$$

where the strict inequality follows from using again (13). So it is *strictly* better to choose action 1 over action 2 if we are in s_1 and have had a return x so far.

We conclude from both cases that there is no optimal Markovian policy.

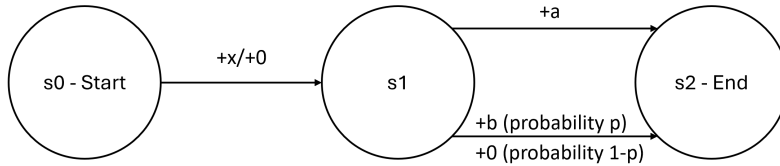


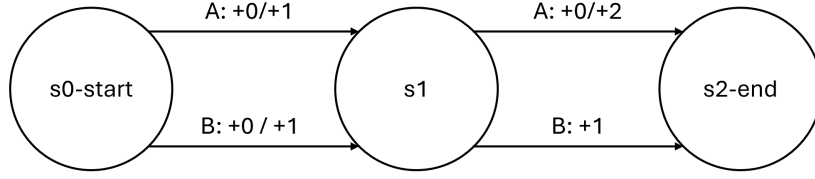
Figure 11: MDP serving as counterexample for the proof of the last implication. While this example has random rewards, another counterexample with random transitions and deterministic rewards can be designed, in the same way as in Remark 11.

G.5 Proof of Proposition 5

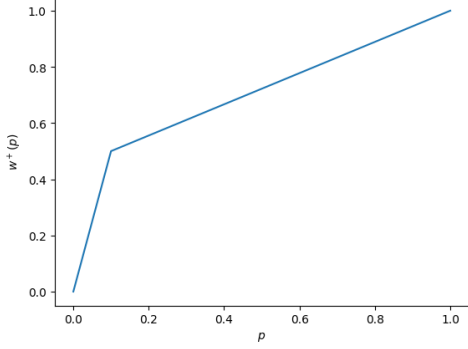
We proceed in the same way as for Proposition 2 by providing a counterexample. We consider the utility function $\mathcal{U} : x \mapsto 1 - \exp(-\beta x)$ with $\beta = \frac{1}{2}$, and the same w^+ function as in the proof of Proposition 2:

$$w^+(x) = \begin{cases} 5x & \text{if } x \leq 0.1, \\ \frac{1}{2} + \frac{5}{9}(x - 0.1) & \text{otherwise.} \end{cases}$$

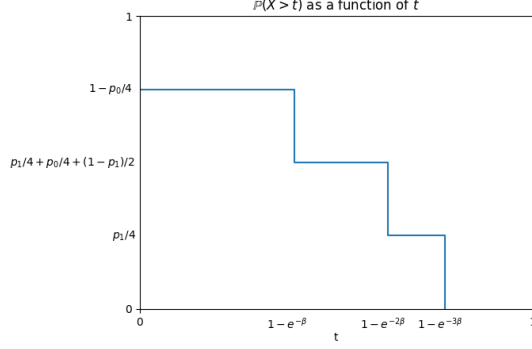
We also set $w^- = 0$. However, we consider another MDP. Our MDP has three states: an initial state s_0 , an intermediate state s_1 , and a terminal state s_2 . There are two actions: A and B. All trajectories start in s_0 . Any action from s_0 leads to s_1 with probability 1 and yields reward +1 with probability $\frac{1}{2}$ and 0 otherwise. The action taken when in s_0 is completely irrelevant. Any action taken in s_1 leads to s_2 with probability 1 and the episode stops as soon as s_2 is reached. When taking action A in s_1 , the reward is either 0 or +2, with probability $\frac{1}{2}$ each. When taking action B in s_1 , the reward is +1 with probability 1. All policies in Π_{NM} can be described by $(p_{\text{start}}, p_0, p_1)$, where p_{start} is the probability of choosing action A when in s_0 , p_0 is the probability of choosing action A in s_1 if the transition from s_0 to s_1 yielded reward 0 and p_1 is the probability of choosing action A in s_1 if the transition from s_0 to s_1 yielded reward 1. p_{start} is irrelevant to the performance of the policy so we can ignore it. The set of Markovian policies here is the set of policies such as $p_0 = p_1$. $\mathbb{C}(\pi)$ is a piecewise affine function of p_0 and p_1 and it can therefore be directly maximized. We omit the calculations here: one can check that the best achievable CPT value for Markovian policies is ≈ 0.616 for $p_0 = p_1 = 0.4$ but that a CPT value of ≈ 0.625 is achievable for $p_0 = 0$ and $p_1 = 0.4$, proving the lemma.



(a) The MDP



(b) The w^+ function



(c) The $t \mapsto \mathbb{P}(X > t)$ function

Figure 12: Figures for the proof of Proposition 5

H Proofs and Additional Details for Section 4

H.1 Proof of Theorem 6

The CPT value is a difference between two integrals (see definition in (1)). In what follows, we compute the derivative of the first integral assuming that the second one is zero in the CPT value. A similar treatment can be applied to the second integral. We skip these redundant details for conciseness.

Remark 13. *As we consider a finite horizon setting with finite state and action spaces, the integral on trajectories τ are in fact finite sums, allowing us to differentiate freely. We still write the proof with \int signs, signalling our hope that, under some technical assumptions, our proof could be generalized to a setting with infinite horizon and/or infinite state and action spaces.*

Using the shorthand notation $X = \sum_{t=0}^{H-1} r_t$, we first observe that:

$$\mathbb{C}(X) = \int_{z=0}^{+\infty} w(\mathbb{P}(U(X) > z)) dz = \int_{z=0}^{+\infty} w \left(\int_{\tau \text{ such as } U(R(\tau)) > z} \rho_{\theta}(\tau) d\tau \right) dz, \quad (16)$$

where ρ_{θ} is the trajectory probability distribution induced by the policy π_{θ} defined for any H -length trajectory $\tau = (s_0, a_0, \dots, s_{H-1}, a_{H-1})$ as follows:

$$\rho_{\theta}(\tau) = p(s_0) \prod_{t=0}^{H-1} \pi_{\theta}(a_t | h_t) p(s_{t+1} | h_t, a_t). \quad (17)$$

Remark 14. *Recall that we have ignored the second integral in the CPT value definition for conciseness.*

Starting from the above expression (16), it follows from using the chain rule that:

$$\nabla_{\theta} \mathbb{C}(X) = \int_{z=0}^{+\infty} w'(\mathbb{P}(\mathcal{U}(X) > z)) \nabla_{\theta} \left(\int_{\tau \text{ such as } \mathcal{U}(R(\tau)) > z} \rho_{\theta}(\tau) d\tau \right) dz \quad (18)$$

$$= \int_{z=0}^{+\infty} w'(\mathbb{P}(\mathcal{U}(X) > z)) \int_{\tau \text{ such as } \mathcal{U}(R(\tau)) > z} \nabla_{\theta} \rho_{\theta}(\tau) d\tau dz \quad (19)$$

$$= \int_{\tau} \int_{z=0}^{\mathcal{U}(R(\tau))} w'(\mathbb{P}(\mathcal{U}(X) > z)) \nabla_{\theta} \rho_{\theta}(\tau) dz d\tau \quad (20)$$

$$= \int_{\tau} \phi(\mathcal{U}(R(\tau))) \nabla_{\theta} \rho_{\theta}(\tau) d\tau, \quad (21)$$

where $\phi(t) := \int_{z=0}^t w'(\mathbb{P}(\mathcal{U}(X) > z)) dz$ for any real t .

We now use the standard log trick to rewrite our integral as an expectation:

$$\nabla_{\theta} \mathbb{C}(X) = \int_{\tau} \phi(\mathcal{U}(R(\tau))) \rho(\tau) \nabla_{\theta} \log \rho(\tau) d\tau = \mathbb{E}_{\tau \sim \rho} [\phi(\mathcal{U}(R(\tau))) \nabla_{\theta} \log \rho(\tau)].$$

Furthermore, we can expand the gradient of the score function using (17) as follows:

$$\log \rho_{\theta}(\tau) = \log p(s_0) + \sum_{t=0}^{H-1} \log \pi_{\theta}(a_t | h_t) + \sum_{t=0}^{H-1} \log p(s_{t+1} | h_t, a_t), \quad (22)$$

$$\nabla_{\theta} \log \rho_{\theta}(\tau) = \sum_{t=0}^{H-1} \nabla_{\theta} \log \pi_{\theta}(a_t | h_t), \quad (23)$$

where the last step follows from observing that only the policy terms involve a dependence on the parameter θ . Combining (21) and (23) leads to our final policy gradient expression:

$$\nabla_{\theta} \mathbb{C}(X) = \mathbb{E} \left[\phi \left(\sum_{t=0}^{H-1} r_t \right) \sum_{t=0}^{H-1} \nabla_{\theta} \log \pi_{\theta}(a_t | h_t) \right]. \quad (24)$$

Note that we have used the notation ϕ above instead of φ used in Theorem 6 to avoid the confusion with the full definition of φ which involves both integrals.

H.2 Alternative Practical Procedure for Computing Stochastic Policy Gradients

In this section, we discuss an alternative approximation procedure to the one proposed in section 4 for computing stochastic policy gradients. More precisely, we seek to approximate $\varphi(R(\tau))$ without the need for estimating quantiles and using order statistics for this. This alternatively procedure will be especially useful in practice when the probability distortion w is not necessarily differentiable or smooth. As discussed in the main part, one of the key challenges to compute stochastic policy gradients is to compute the integral terms appearing in the policy gradient expression. Our idea here is to approximate the probability distortion function w by a piecewise (linear or quadratic) function, leveraging the following useful lemma which shows that the integral is simple to compute when w is quadratic for instance.

Lemma 15. *Let X be a real-valued random variable and suppose that the weight function w is quadratic on an interval $[a, b]$ for some positive constants a, b , hence there exist $\alpha, \beta \in \mathbb{R}$ s.t. for all $x \in [a, b]$, $w'(x) = \alpha x + \beta$. Let $Y_{a,b} := \min(\max(\mathcal{U}(X) - a, b - a), 0)$. Then, we have that $\int_a^b w'(\mathbb{P}(\mathcal{U}(X) > z)) dz = \alpha \mathbb{E}[Y_{a,b}] + \beta(b - a)$.*

Proof. For any $a, b \in \mathbb{R}$ s.t. $a \leq b$, we have

$$\begin{aligned}
\int_a^b w'(\mathbb{P}(\mathcal{U}(X) > z)) dz &= \int_0^{b-a} w'(\mathbb{P}(\mathcal{U}(X) - a > v)) dv \\
&= \int_0^{b-a} (\alpha \mathbb{P}(\mathcal{U}(X) - a > v) + \beta) dv \\
&= \alpha \int_0^{b-a} \mathbb{P}(\mathcal{U}(X) - a > v) dv + \beta(b-a) \\
&= \alpha \int_0^{b-a} \mathbb{P}(Y_{a,b} > v) dv + \beta(b-a) \\
&= \alpha \int_0^{+\infty} \mathbb{P}(Y_{a,b} > v) dv + \beta(b-a) \\
&= \alpha \mathbb{E}[Y_{a,b}] + \beta(b-a).
\end{aligned}$$

□

This result is convenient: Instead of estimating an entire probability distribution, we just have to estimate an expectation, which is much easier. However, we cannot reasonably approximate an arbitrary weight function by a quadratic function. Therefore, we consider the larger class of piecewise quadratic functions for which Lemma 15 extends naturally.

Proposition 16. *Let w be piecewise quadratic: there exists $q_1 < q_2 < \dots < q_k$, with $q_1 = 0$ and $q_k = 1$, as well as reals $\alpha_1, \dots, \alpha_k, \beta_1, \dots, \beta_k$ and $\delta_1, \dots, \delta_k$ such as $w(x) = \sum_{i=1}^{k-1} \mathbb{1}_{[q_i, q_{i+1}[}(t) (\frac{1}{2} \alpha_i t^2 + \beta_i t + \delta_i)$. For all $1 \leq i \leq k-1$, define the i -th quantile of $\mathcal{U}(X)$ as $\tilde{q}_i := \sup\{t \in \mathbb{R} \cup \{+\infty, -\infty\}, \mathbb{P}(\mathcal{U}(X) > t) \geq q_i\}$. Then, for any given $t \in [\tilde{q}_{j+1}, \tilde{q}_j[$:*

$$\int_0^t w'(\mathbb{P}(\mathcal{U}(X) > z)) dz = \sum_{i=j+1}^{k-1} (\alpha_i \mathbb{E}(Y_{\tilde{q}_{i+1}, \tilde{q}_i}) + \beta_i (\tilde{q}_i - \tilde{q}_{i+1})) + \alpha_j \mathbb{E}(Y_{\tilde{q}_j, t}) + \beta_j (t - \tilde{q}_{j+1}).$$

Proof. We simply apply Lemma 15 to each segment:

$$\begin{aligned}
\int_0^t w'(\mathbb{P}(\mathcal{U}(X) > z)) dz &= \sum_{i=j+1}^{k-1} \int_{\tilde{q}_{i+1}}^{\tilde{q}_i} w'(\mathbb{P}(\mathcal{U}(X) > z)) dz + \int_{\tilde{q}_{j+1}}^t w'(\mathbb{P}(\mathcal{U}(X) > z)) dz \\
&= \sum_{i=j+1}^{k-1} (\alpha_i \mathbb{E}(Y_{\tilde{q}_{i+1}, \tilde{q}_i}) + \beta_i (\tilde{q}_i - \tilde{q}_{i+1})) + \alpha_j \mathbb{E}(Y_{\tilde{q}_j, t}) + \beta_j (t - \tilde{q}_{j+1}).
\end{aligned}$$

□

The above lemma shows that we would have to estimate several quantiles and expectations to use this result. In particular, the expectation $\mathbb{E}(Y_{\tilde{q}_j, t})$ introduces some undesired computational complexity as the term differs for every t . However, if we rather consider a simpler piecewise affine approximation of w which can be computed once before any computation (independently from the rest) if the probability distortion function w is priorly known (which we implicitly suppose throughout this work), the expression is greatly simplified, yielding Lemma 17.

Lemma 17. *Suppose that the weight function $w : [0, 1] \mapsto [0, 1]$ is piecewise affine, i.e. there exists $q_1 < q_2 < \dots < q_k$, with $q_1 = 0$ and $q_k = 1$, as well as reals β_1, \dots, β_k and $\delta_1, \dots, \delta_k$ s.t. $w(x) = \sum_{i=1}^{k-1} \mathbb{1}_{[q_i, q_{i+1}[}(x) (\beta_i x + \delta_i)$ for any $x \in [0, 1]$. Let $\tilde{q}_i := \sup\{t \in \mathbb{R} \cup \{+\infty, -\infty\}, \mathbb{P}(\mathcal{U}(X) > t) \geq q_i\}$ for any $i = 1, \dots, k$. Then for any $1 \leq j \leq k-1$ and any $t \in [\tilde{q}_{j+1}, \tilde{q}_j[$,*

$$\int_0^t w'(\mathbb{P}(\mathcal{U}(R(\tau)) > z)) dz = \sum_{i=j+1}^{k-1} (\beta_i (\tilde{q}_i - \tilde{q}_{i+1})) + \beta_j (t - \tilde{q}_{j+1}).$$

Environment	Utility function	w^+ function	Figure	Comment
Grid	Various	3-segment piecewise affine function	Fig. 2 and Apdx I.4	We observe convergence and various behaviours for various utility functions
Traffic Control	Identity	Risk averse (w_{ra})	Apdx. I.5	The policy goes around the city center
Traffic Control	Identity	Risk neutral (Id.)	Apdx. I.5	The policy goes through the city center
Traffic Control	Identity	Risk averse (w_{ra}) / Risk-neutral (Id.)	Apdx. I.5	Same behavior, entropy regularization needed
Scalable Grid	Identity	Risk-averse (w_{ra})	Fig. 3	Our algorithm converges faster than CPT-SPSA-G for large grids
Electricity Management	Identity	Very risk averse (w_{vra}) / Very risk seeking (w_{vrs}) / Risk-neutral (Id.)	Fig. 2	Convergence to different reward distributions in accordance to behavior to risk
Fig. 16	Exponential, Kahneman-Tversky	Risk-neutral (Id.)	Fig. 21	The result illustrates Theorem 4
Fig. 14a	Identity	Risk-seeking (w_{rs})	Fig. 15	The result illustrates Proposition 2

Table 2: Summary of experiments

I More Details about Section 5 and Additional Experiments

Table 2 recaps the various experimental settings. The risk-neutral w^+ function is simply the identity function. As for the definition of other probability distortion functions w^+ we use for experiments, we define:

$$\begin{aligned}
 w_{ra}(x) &:= \begin{cases} 0.5x & \text{if } x \leq 0.9, \\ 5.5x - 4.5 & \text{otherwise.} \end{cases} & w_{rs}(x) &:= \begin{cases} 5x & \text{if } x \leq 0.1, \\ \frac{1}{2} + \frac{5}{9}(x - 0.1) & \text{otherwise.} \end{cases} \\
 w_{sra}(x) &:= \begin{cases} 0.1x & \text{if } x \leq 0.9, \\ 9.1x - 8.1 & \text{otherwise.} \end{cases} & w_{srs}(x) &:= \begin{cases} 9x & \text{if } x \leq 0.1, \\ \frac{1}{9}x + \frac{8}{9} & \text{otherwise.} \end{cases}
 \end{aligned}$$

Instead of vanilla stochastic gradient descent, we use the Adam optimizer to speed up convergence. In our Python implementation, we use the same batch of trajectories for estimating the function φ and for the performing the stochastic gradient ascent step. We have run the experiments on a laptop with a 13th Gen Intel Core i7-1360P 2.20 GHz CPU and 32 GB of RAM.

We use the tanh activation function before the last softmax layer to encourage exploration and reduce the risk of converging to local optima which may occasionally occur for some runs.

I.1 Additional Figure

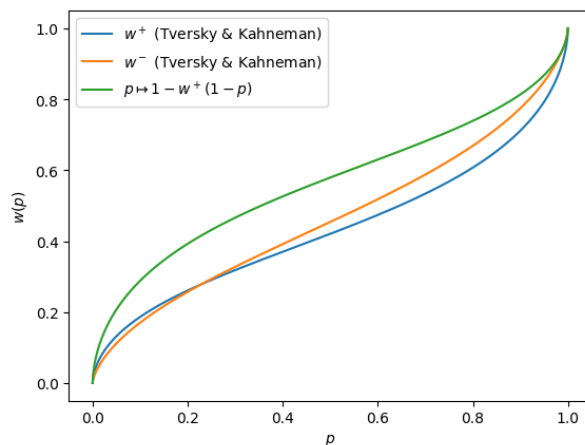


Figure 13: Illustration of the flexibility of CPT compared to the Distortion Risk Measure. Notice how w^- is distinct from both w^+ and $p \mapsto 1 - w^+(1 - p)$.

I.2 Illustration of Proposition 2: about the need for Stochastic Policies in CPT-RL

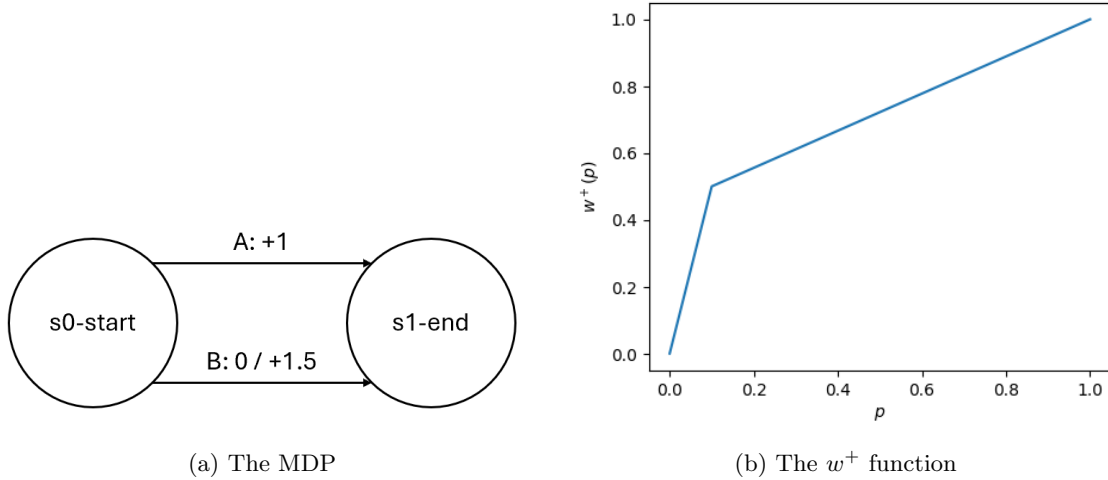


Figure 14: Setting of the experiment on non-deterministic policies and batch size influence

We illustrate Proposition 2 and study experimentally the behavior of our algorithm with regards to small batch sizes.

Setting. We use the barebones setting (Figure 14) introduced in the proof of Proposition 2 with its w function that aggressively focuses on the 10% of favorable outcomes. Denoting by p the probability of choosing A for a given policy, we look at the value of p at convergence (1000 optimization steps) for various batch sizes. The optimal policy corresponds to $p = 0.8$.

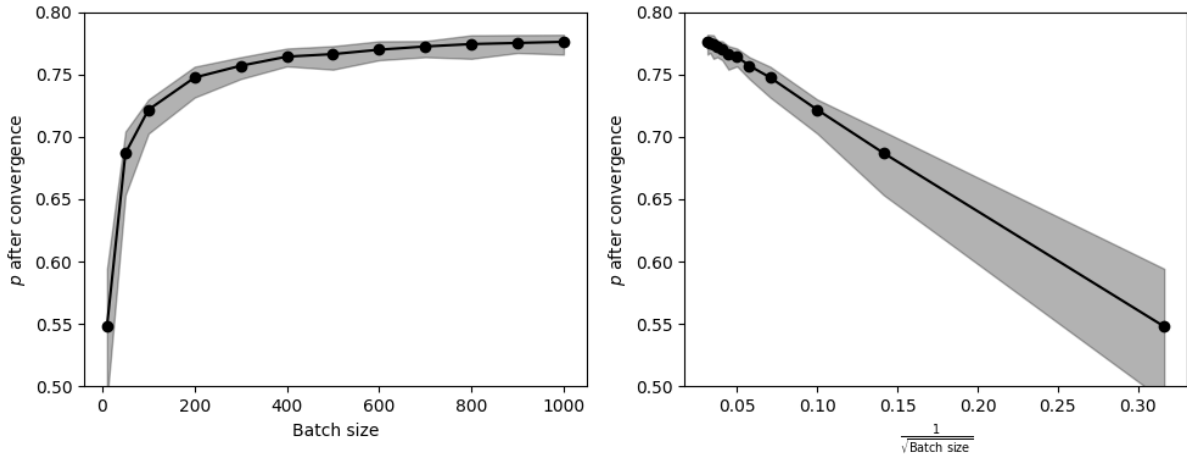


Figure 15: Results of the experiment on non-deterministic policies and batch size influence, over 100 runs. The black dots are the medians and the shaded area represents the interquartile range.

Insights. For each batch size we test, we run and plot a hundred training rounds (Figure 15). We first observe that the policy we obtain with our algorithm indeed approaches the optimal $p = 0.8$ policy. The estimation error (w.r.t. the optimal theoretical value of $p = 0.8$) appears to be of order $\frac{1}{\sqrt{\text{batch size}}}$. It was to be expected that a small batch size would lead to a bias in CPT value and CPT gradient estimation, and, finally, in policy, as a small batch size renders impossible an accurate estimation of the probability distribution of the total return function. The fact that this bias appears to be proportional to the inverse of the square root of the batch size is in line with the standard statistical intuition (as e.g.

per the central limit theorem). In our particular example, the estimated p is below (and not above) the theoretical p . This is likely because our w function places a strong weight on the top 10% of outcomes. Hence there is an imbalance between the impact of overestimating and underestimating the proportion of good outcomes in a given run: if we underestimate the probability of getting $+1.5$ with a given policy due to sampling, the effect will be stronger than the opposite effect we would get by overestimating the probability of the same error. As the batch size grows, the estimation error is reduced and the effect vanishes.

I.3 Illustration of Theorem 4: Markovian vs Non-Markovian Policies for CPT-RL

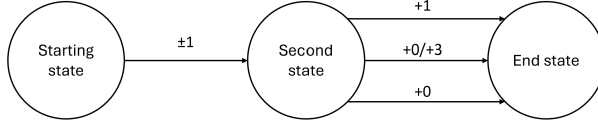


Figure 16: The environment for the experiment on non-Markovian policy

To illustrate the fundamental difference between memoryless utility functions studied in Theorem 4 and the others we conduct a small experiment on a simple setting (Figure 16), similar to the one introduced in the proof of the theorem. We consider three states and three actions. From the starting state, any action leads to the second state with probability 1 and yields a reward of $+1$ with probability $\frac{1}{2}$ and of -1 with probability $\frac{1}{2}$. Once in the second state, the first action yields reward $+1$ with probability 1, the second action yields 0 or 3 with probability $\frac{1}{2}$ each, and the third action always yields 0. We compare the performance of a policy parametrized in $\Pi_{\Sigma, NS}$ and one in $\Pi_{M, NS}$.

Insights. The results (Figure 21) illustrate indeed the performance advantage of the non-Markovian policy compared to the Markovian one in the case of a non-affine, non-exponential utility function, and the absence thereof in the exponential setting.

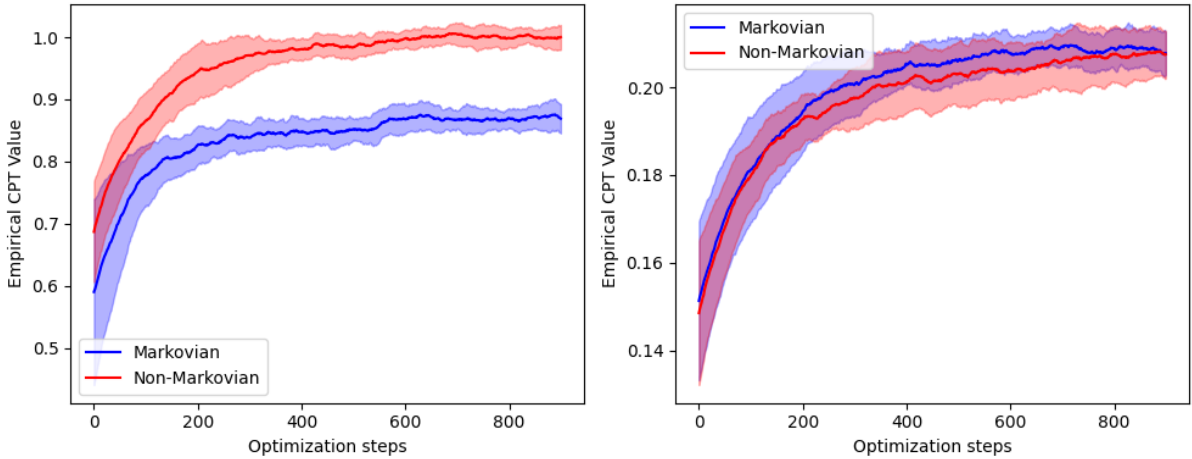


Figure 17: Comparison of Markovian and Non-Markovian policy performances for non-exponential (left) and exponential (right) utility functions. Shaded areas represent a range of \pm one standard deviation over 20 runs.

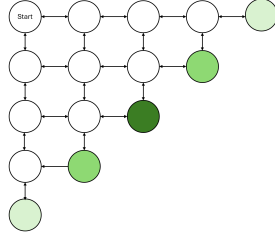


Figure 18: Scaling grid example.

I.4 Grid Environment

↓	↓	↓	↓
→	↓	↓	↓
→	→	→	↓
+5	→	→	+6

(a) A risk-neutral optimal policy obtained with our algorithm

↓	↓	↓	↓
↓	↓	↓	↓
↓	→	→	↓
+5	→	→	+6

(b) An optimal policy obtained by training with the risk-averse utility $\mathcal{U} : x \mapsto \sqrt{x}$

Figure 19: Comparison of optimal policies under risk-neutral and risk-averse scenarios

Exploration. To avoid our gradient ascent algorithm getting stuck in a local optimum, we have to ensure enough exploration is going on. Therefore, we tweak the last layer of the neural network to prevent every action’s probability from vanishing too soon. We choose a parameter α , choose our last layer as $x \mapsto \text{softmax}(\alpha \tanh(x/\alpha))$, and we let α slowly grow with the iterations. A small α forces exploration, larger α allows for more exploitation: this is similar to an ϵ -greedy scheme (with ϵ decaying as α grows), as it forces every action to be chosen with at least a small probability.

Scalability to larger state spaces. We consider a family of MDPs where the state space is a $n \times n$ grid for a given integer parameter n . The agent starts in the top right corner and has always four possible actions (up,down,left,right). Taking a step yields a reward of $\frac{-1}{n}$, attempting to leave the grid yields $\frac{-2}{n}$, and reaching the anti-diagonal ends the episode with a positive reward. All cells on the anti-diagonal yield the same expected reward, but with different levels of risk; the least risky reward is the deterministic one, in the center of the grid. We consider tabular policies and the initial policy is a random policy assigning the probability 1/4 to each action. We test the sensitivity of the performance of both algorithms to the size of the state space. The steps sizes of both algorithms have been tuned to approach their possible performance; we wish to draw attention not to the absolute performance of either algorithm on any particular example, but rather to the evolution of the performance of both as the size of the problem increases. We observe that the performance of CPT-SPSA-G suffers for larger state space size whereas our PG algorithm is robust to state space scaling. While both algorithms are gradient ascent based algorithms in principle, our stochastic policy gradients are different.

Influence of the utility function. We consider a 4x4 grid for our illustration purpose. Our agent starts on a random square on one of the three upper rows of the grid, and can move in all four directions. Any move to an empty square will award it a random reward of -1 with probability $\frac{1}{2}$ and of $+0.8$ with probability $\frac{1}{2}$. Therefore, longer trajectories are slightly costly in expectation, and generate significant variance. In two corners of the grid, we add cells that yields rewards of $+5$ for one or $+6$ for the other, and conclude the episode. Illegal moves (attempting to leave the grid) are punished by a negative reward. Our parameterized policy is a neural network whose last layer is activated with softmax and has 4 coordinates corresponding to the 4 different possible moving actions. We consider solving (CPT-PO) with different utility functions: risk-neutral identity utility, risk-averse KT utility, as well as exponential utility function. The obtained policies differ depending on the utility function. For examples of risk-neutral/averse policies obtained, see Fig. 19b.

I.5 Traffic Control

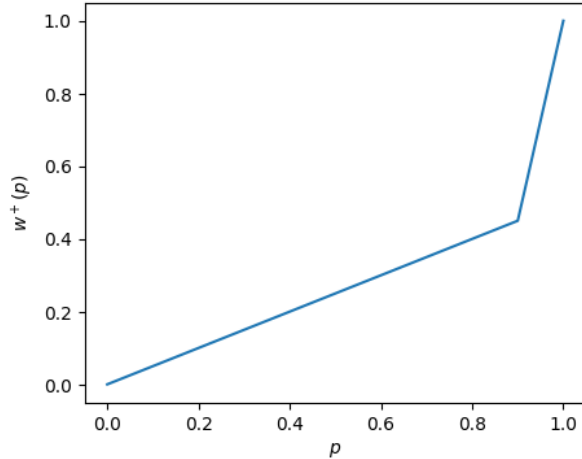


Figure 20: The probability distortion function w^+ used for the traffic control experiment.

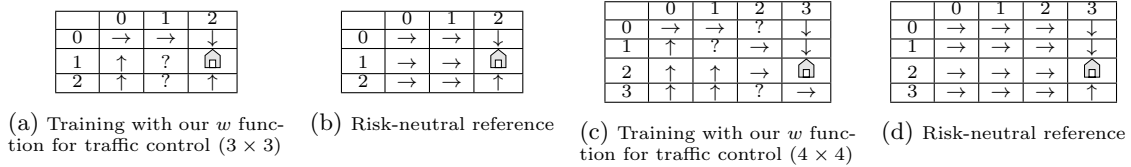


Figure 21: Examples of policies obtained with our algorithm. Question marks indicate a non-deterministic action selection in a given state.

Implementation details. In both cases, the risk-neutral optimal solution (going around the city center) is also a local optimum for the risk-averse objective, and, because it is a shorter path, is easier to stumble upon by chance when exploring the MDP. This means we have to implement special measures to force exploration. The algorithm used *as is* is prone to get stuck from time to time in local minima on this example. It would seem that our w function, which is aggressively risk-averse, hinders exploration. To mitigate this, we introduce an entropy regularization term that we add to the score function with a decaying regularization weight in the policy gradient found in Theorem 6, see appendix I for further details. We incorporate entropy regularization in the policy gradient as follows:

$$\mathbb{E} \left[\varphi \left(\sum_{t=0}^{H-1} r_t \right) \sum_{t=0}^{H-1} \nabla_{\theta} \left(\log \pi_{\theta}(a_t | s_t) + \underbrace{\alpha_n H(\pi_{\theta}(a_t | s_t))}_{\text{Entropy regularization term}} \right) \right], \quad (25)$$

where α_n is the weight of the regularization. We found that a decaying α_n yielded the best results.

On the 4×4 grid, we also start by pretraining our model with a risk-neutral method for a few steps, to accelerate training and avoid some bad local optima we can stumble upon due to unlucky policy initialization, before carrying on with our risk-aware method.

I.6 Electricity Management

Public data is available online.⁵

We consider an electricity management system for an individual home which has solar panels for producing electricity and a battery for storing energy. The intensity of the solar panel’s electricity production follows a sinusoidal function during daytime hours and vanishes at night. The home consumes

⁵www.services-rte.com/en/view-data-published-by-rte/france-spot-electricity-exchange.html

a random and varying amount of electricity and can buy and sell electricity to the outer grid. The selling price varies during the day whereas the buying price is fixed and significantly higher than the selling prices. We use public data for selling prices recorded on a national electricity network. We consider a 24h time frame starting at 6 am and we divide the day into twelve two-hour time slots. For each time slot, the agent has to decide how much to buy or sell to the grid given the production, the battery’s charge, the price on the market and the consumption. We run the algorithm with three different objectives, changing the w function: a risk-neutral one, a risk-averse one and a risk-seeking one (see Table 2). We consider a Gaussian policy in which the mean is parameterized by a neural network. We report the results for running our algorithm in Fig. (2) (right). The most rewarding time to sell our electricity is around 4pm (see electricity prices in appendix I.6, Fig. 22, right). However, selling too much too soon exposes us to the risk of falling short of battery during the night and risking to buy it later for a higher price.

The risk-averse policy avoids selling a lot of electricity and tends to keep it stored until the end of the day. Conversely, the risk-seeking policy aggressively sells energy when the markets are high at the cost of possibly having to buy it again later in the day. We can see on Fig. 2 (right), where we plot the distribution of total returns for various trained models with different w functions and a few different random initializations each, that, as we would wish to see, the risk-averse policy has the distribution with the best left tail (worst cases are not too bad), the risk-seeking distribution has the best right tail (best cases are particularly good). The risk-neutral policy has the best mean value.

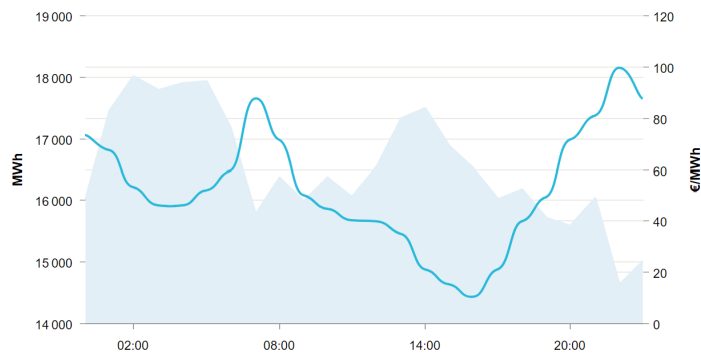


Figure 22: Electricity prices in a typical day, the blue line (right-hand side scale) records the electricity price on the European market, the shaded area (left-hand side scale) represents the total electricity production in France.

I.7 Trading in Financial Markets

We discuss here an application of our methodology to financial trading. The goal is to train RL trading agents using our general PG algorithm in the setting of our CPT-RL framework.

Environment: general description. We consider a gym trading environment available online, all the details about this environment are available here: <https://gym-trading-env.readthedocs.io/en/latest/>. This environment simulates stocks and allows to train RL trading agents. For the interest of the reader, we provide a brief summary explaining how the environment works. The environment is build from a given dataframe and a list of possible positions. The dataframe contains market data throughout a given period. The list of possible positions will represent the set of possible actions the agent can take, We provide more details about our specific environment in the following paragraph.

Our trading environment. We use data from the Bitcoin USD (BTC-USD) market between May 15th 2018 and March 1st 2022 available in the aforementioned website. We note that the data used follows the same pattern as publicly available data after a few preprocessing steps, the reader can find such data examples at <https://finance.yahoo.com/quote/BTC-USD/history> including the date, a few extracted features ('open', 'high', 'low', 'close') which respectively represent the open price, i.e. the price at which the first trade occurred for the asset at the beginning of the time period, the highest, lowest and last such prices, and the volume in USD which is the total value of all trades executed in a given time period. In particular, we will consider static features (computed once at the beginning of the data frame preprocessing) and dynamic features (computed at each time step) such as the last position taken as introduced by the Gym Trading Environment.

- **State space:** We consider a seven dimensional continuous state space. Features are constructed from the raw stock market data as previously explained. State transitions are described using the provided time series. See the publicly available code of the environment for more details.
- **Action space:** We consider three classical types of positions the trader can take in a financial market: SHORT, OUT and LONG. These positions constitute the set of actions. These actions refer to whether the trader expects the price of an asset to rise or fall and how they are positioned to profit from that fluctuation. Extending this setting to a setting with a larger set of positions is straightforward as the environment implementation also supports more complex positions.
- **Rewards:** The rewards we consider are given by the log values of the ratio of the portfolio valuations at times t and $t - 1$. Borrowing interest rates and trading fees are also considered in the computation. The reward function can also be easily modified in the environment thanks to the implementation of the Gym Trading Environment which builds on the standard Gym environments.

Remark 18. *One can easily build their own environment by downloading their own dataframe for any historical stock market data and performing their desired preprocessing as for the features they would like to consider to build their states.*

Experimental setting. We have tested several utility and probability weighting functions including a risk averse exponential of the form $x \mapsto \frac{1}{\beta}(1 - \exp(-\beta x))$ with different values of β as well as the KT (Kahneman and Tversky) function as defined in the main part with different values of the reference point x_0 to illustrate its influence.

Hyperparameters. We used the following set of parameters to conduct the experiments:

Table 3: Hyperparameters

Hyperparameter	Value
Optimizer	Adam
Learning rate	0.05
Number of episodes	100
Batch size	5
Number of steps per episode	25

Additional hyperparameters used are directly reported in the legends of the figures below.

Results. We refer the reader to Fig. 23 and Fig. 24 below. We make a few observations:

- Influence of the reference point: It can be seen that the reference point shifts the values of the achieved CPT returns: The smaller the reference point, the larger are the returns. This is because only values larger than the reference point are perceived as positive returns given the definition of the KT utility. This illustrates how the subjective perception of the agent of the returns is taken into account by the model.
- Different return trajectories for different risk averse functions: Different values of β lead to different trajectories overall which can translate to different levels of risk aversion. In particular, the curves do not match the identity utility case in the first episodes and show more or less risk taken towards optimizing the CPT returns.
- Influence of the parameter α in KT’s utility (Fig. 24): Observe that the exponent α in the utility distorts the function and shifts the returns significantly. Lower values of α lead to higher returns in this setting where the returns (as per the ratio definition of the reward) are smaller than 1. This parameter α provides a degree of freedom to model the behavior of the agent as per their perception of the returns. Different values of α modify the curvature of the utility function (w.r.t. the reference point which is $x_0 = 0$ here) which is concave for gains and convex for losses.

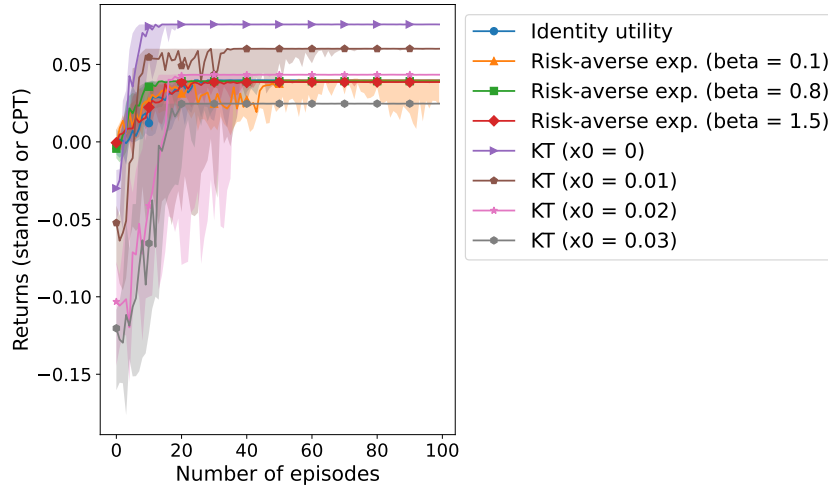


Figure 23: Performance of our PG algorithm on a financial trading application. KT refers to Kahneman and Tversky’s utility function, x_0 is the reference point used in that utility, exp. refers to exponential. Shaded areas are interquartile (25-75%) margins and curves report the median values over 10 different runs.

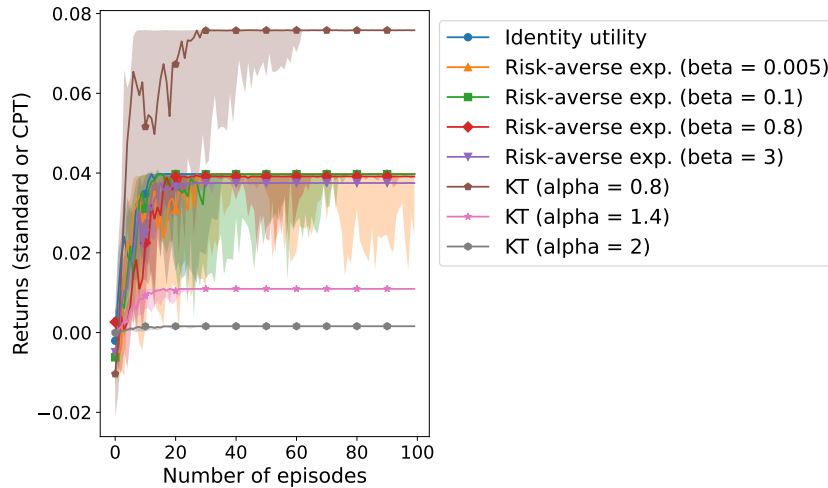


Figure 24: Performance of our PG algorithm on the same financial trading application. KT refers to Kahneman and Tversky’s utility function, alpha is the parameter used in the definition of KT’s utility, exp. refers to exponential. Shaded areas are interquartile (25-75%) margins and curves report the median values over 10 different runs.

I.8 Control on MuJoCo Environments

In this section we test our algorithm on the INVERTEDPENDULUM-V5 environment [Todorov et al., 2012] to demonstrate that our PG algorithm is also applicable to other control benchmarks with continuous state and action spaces.

Hyperparameters. We used the following set of parameters to obtain our results:

Table 4: Hyperparameters

Hyperparameter	Value
Optimizer	Adam
Learning rate	1e-4
Number of episodes	2000
Batch size	32
Maximum number of steps per episode	200

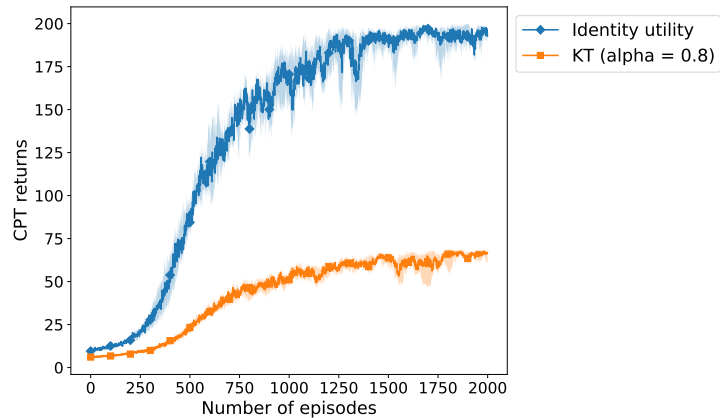


Figure 25: Performance of our PG algorithm on the INVERTEDPENDULUM-V5 environment [Todorov et al., 2012]. KT refers to Kahneman and Tversky’s utility function, α is the parameter used in the definition of KT’s utility, $\exp.$ refers to exponential. Shaded areas are interquartile (25-75%) margins and curves report the median values over 10 different runs. All the CPT return curves are obtained with the same probability weighting function w which is piecewise affine with three segments (hence different from the standard RL identity setting).

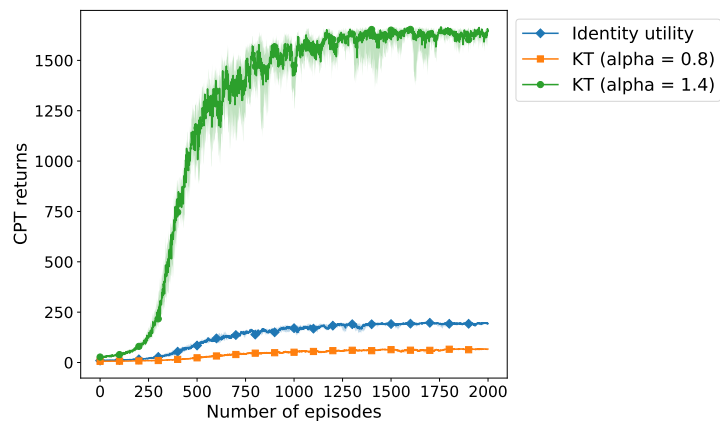


Figure 26: Performance of our PG algorithm on the INVERTEDPENDULUM-V5 environment [Todorov et al., 2012]. This figure complements Fig 25 with the CPT returns using a KT utility with $\alpha = 1.4$. Notice that a much higher CPT return is achieved in that case. We also provide Fig. 25 for scaling purposes, the CPT returns being much higher for KT ($\alpha = 1.4$).